AD_____

Award Number: DAMD17-03-1-0006

TITLE: Disruption of Fibroblast Growth Factor Receptor (FGFR) Signaling as an Approach to Prostate Cancer Therapy

PRINCIPAL INVESTIGATOR: Mustafa Ozen, Ph.D.

CONTRACTING ORGANIZATION: Brigham and Women's Hospital
Boston, MA 02115

REPORT DATE: April 2005

TYPE OF REPORT: Annual

PREPARED FOR: U.S. Army Medical Research and Materiel Command
Fort Detrick, Maryland 21702-5012

DISTRIBUTION STATEMENT: Approved for Public Release;
Distribution Unlimited

REPORT DOCUMENTATION PAGE

Form Approved
OMB No. 074-0188

1. AGENCY USE ONLY (Leave blank)	2. REPORT DATE	3. REPORT TYPE AND DATES COVERED
	April 2005	Annual (1 Apr 2004 - 31 Mar 2005)

4. TITLE AND SUBTITLE
Disruption of Fibroblast Growth Factor Receptor (FGFR) Signaling as an Approach to Prostate Cancer Therapy

5. FUNDING NUMBERS
DAMD17-03-1-0006

6. AUTHOR(S)
Mustafa Ozen, Ph.D.

7. PERFORMING ORGANIZATION NAME(S) AND ADDRESS(ES)
Brigham and Women's Hospital
Boston, MA 02115

E-Mail: mozen@bcm.tmc.edu

8. PERFORMING ORGANIZATION REPORT NUMBER

9. SPONSORING / MONITORING AGENCY NAME(S) AND ADDRESS(ES)
U.S. Army Medical Research and Materiel Command
Fort Detrick, Maryland 21702-5012

10. SPONSORING / MONITORING AGENCY REPORT NUMBER

11. SUPPLEMENTARY NOTES

12a. DISTRIBUTION / AVAILABILITY STATEMENT
Approved for Public Release; Distribution Unlimited

12b. DISTRIBUTION CODE

13. ABSTRACT (Maximum 200 Words)

Prostate cancer cells express multiple types of FGF receptor and increased expression of FGF receptor-1 (FGFR-1) is present in poorly differentiated human prostate cancers *in vivo*. We have proposed to evaluate biological affects of DN FGFR expression in human primary prostate epithelial cells and prostate cancer cell lines. The findings in this report support that prostate cancer cells are dependent upon FGFR signaling for survival and cells treated with DN FGFR are arrested G2/M phase of cell cycle followed by cell death. FGF signaling modulated *CDC25C* activity in prostate cancer, and in this manner can promote progression through the G2/M checkpoint. *CDC25C* protein is upregulated in comparison to normal prostate tissue and is present almost exclusively in its active dephosphorylated form. Determining other molecules involved in this pathway contributing tumor growth and survival will facilitate the development of cancer therapies to target FGF signaling pathway

14. SUBJECT TERMS
Growth factors, fibroblast growth factors, fibroblast growth factor receptors, prostate cancer therapy, cell cycle

15. NUMBER OF PAGES
51

16. PRICE CODE

17. SECURITY CLASSIFICATION OF REPORT	18. SECURITY CLASSIFICATION OF THIS PAGE	19. SECURITY CLASSIFICATION OF ABSTRACT	20. LIMITATION OF ABSTRACT
Unclassified	Unclassified	Unclassified	Unlimited

Table of Contents

INTRODUCTION:

Alterations in Fibroblast Growth Factor (FGF) signaling pathway have been implicated in the pathogenesis of variety of malignancies including prostate cancer by *in vitro* and *in vivo* studies[Polnaszek et al., 2003;Ozen et al., 2001;Takahashi, 1998;Giri et al., 1999]. FGFs produce their mitogenic and angiogenic effects in target cells by signaling through four distinct cell-surface tyrosine kinase receptors, FGFR-1 through FGFR-4. Prostate epithelial cells express FGF receptors and require FGFs for growth in primary culture. Prostate cancer cells express multiple types of FGF receptor and increased expression of FGF receptor-1 (FGFR-1) is present in poorly differentiated human prostate cancers *in vivo*[Takahashi, 1998;Giri et al., 1999]. We hypothesized that FGF receptor signaling is essential for viability of human prostate cancer cells and disruption of this signaling via expression of a dominant negative FGF receptor-1 protein in human prostate cancer cells might contribute to the death of cancer cells and can be used as adjuvant to current treatment options especially to radiotherapy since it has been also administered locally. Furthermore, analysis of gene expression profile in FGFR DN transfected cells might help our understanding of how FGFR DN works and the differentially expressed genes determined by microarray analysis can be used as targets for prostate cancer therapy.

BODY:

Task 1: We have proposed to evaluate biological affects of DN FGFR expression in human primary prostate epithelial cells and prostate cancer cell lines. We have obtained different recently established prostate cancer cell lines from other investigators and American Type Culture Collection (ATCC). Among these are 22Rv1[Sramkoski et al., 1999] obtained from ATCC, LAPC4 [Craft et al., 1999] from Dr. Charles Sawyers of University of California, Los Angeles, C4, C4-2 and C4-2B[Thalmann et al., 2000] from Dr. Leland Chung of University of Virginia and MDA PCa 2b [Navone et al., 1997] from Dr. Nora Navone of University of Texas M.D. Anderson Cancer Center. These cell lines have been frozen in liquid nitrogen for further experiments. Normal prostate biopsy specimens were also cultured for the purpose of obtaining primary prostate epithelial cells. All cell lines have been tittered for optimal multiplicity of infection (MOI) to be used in subsequent experiments. Viral particles was used to establish MOIs in cell lines since this has been suggested

Table1. Prostate cancer cell lines and appropriate MOIs used in adenovirus infection

Name of the cell line	Origin	Androgen Status	MOI used (in thousand particles)
DU145	Brain metastasis	insensitive	3
PC3	Bone metastasis	insensitive	4
LNCaP	Lymph node metastasis	sensitive	2.5
22 Rv1	CWR22R	insensitive	5
LAPC4	Bone metastasis	sensitive	2.5
MDA Pca 2b	Bone metastasis	sensitive	6
C4	LNCaP	insensitive	4
C4-2	LNCaP	insensitive	5
C4-2B	LNCaP	insensitive	5

as a reliable approach in the literature [Green et al., 2002;Yotnda et al., 2002]. This data and the phenotypes of the cell lines are summarized in Table 1.

To analyze the affect of DN FGFR in human prostate cell proliferation and/or viability, cells were counted by Coulter counter after 24, 48 and 72 hr of infection with DN FGFR and LacZ. As seen in Figure 1, LAPC4 cells had the most dramatic effect on the inhibition of cell proliferation when infected with DN FGFR adenovirus. Over 90 % of the cells died after 72 hours of infection with DN FGFR; however, there was a 16% increase on the number of cells infected with LacZ as control. MDA Pca 2b cells also showed decreased in the number of proliferating cells after infection with DN FGFR adenovirus as compared to control at all three time points (Figure 1). After 72 hours of infection cells treated with DN FGFR stopped proliferating as contrast to the cells infected with control adenovirus which continued to grow and more than doubled in number in 72 hours. The 22 Rv1 cell line only had significant reduction on the number of proliferating cells after 72 hours of infection.

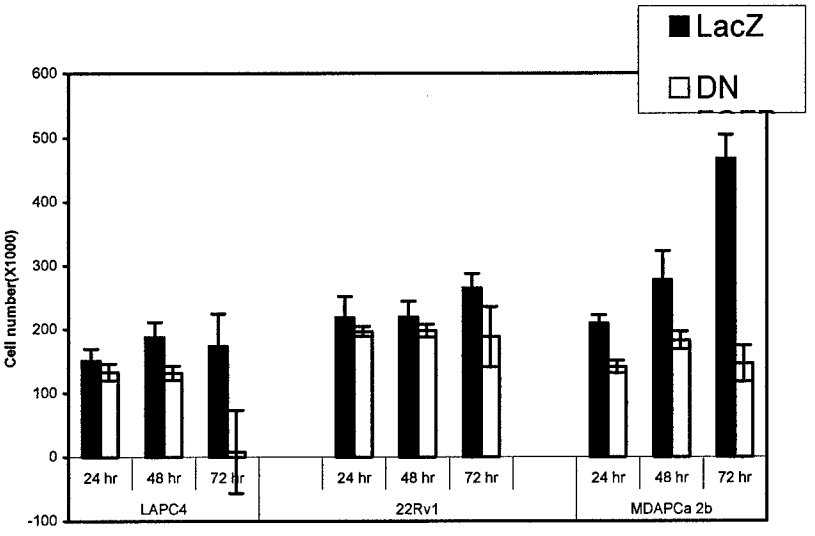

Figure 1. Effect of DN FGFR on prostate cancer cell proliferation and viability. LAPC4 22Rv1 and MDA PCa 2b cells were plated at 5 x 10^4 cells per 35-mm dish and infected with Ad FGFR or Ad Lac Z as control. The cell number was determined by counting with the use of Coulter counter at 24, 48, and 72 hours after infection. All values are the mean of triplicate determinations.

A series of lineage-related LNCaP cell sublines that reflect the various steps of prostate carcinogenesis and progression has been derived[Thalmann et al., 2000]. An androgen-independent (AI) cell line, C4-2, reproducibly and consistently follows the metastatic patterns of hormone-refractory prostate cancer by producing lymph node and bone metastases when injected either s.c. or orthotopically in either hormonally intact or

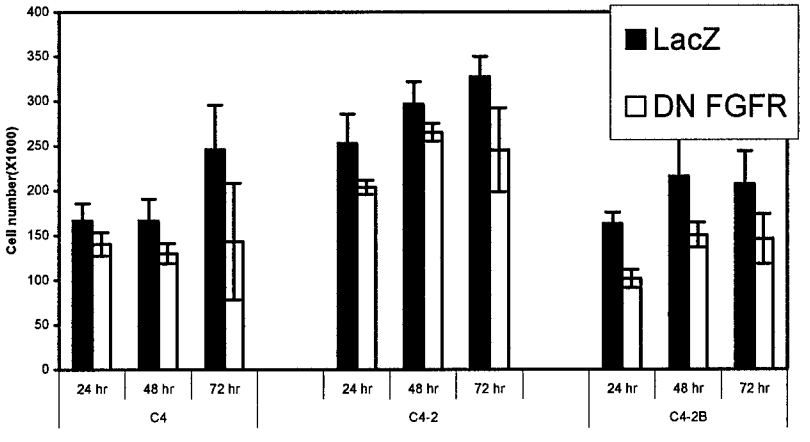

Figure 2. Effect of DN FGFR on prostate cancer cell proliferation and viability on LNCaP prostate cancer sublines C4, C4-2 and C4-2B.

castrated hosts[Thalmann et al., 2000]. This LNCaP model will help improve our understanding of the mechanisms of androgen-dependent to androgen-independent prostate cancer progression. As seen on Figure 2, although DN FGFR adenovirus treatment did decrease the proliferation of all three LNCaP derivatives, The biological effect was not as dramatic as it was in parental LNCap cells. We have previously observed 50- 70% decrease in cell number by 72 hours after DN FGFR treatment [Ozen et al., 2001]. One possible explanation of this difference could be the difference in the endogenous FGF2 responds to the DN FGFR treatment of these cell lines. This possibility is currently under investigation. It is interesting, however, to note that the original LNCaP cell line was androgen sensitive in contrast to C4-2 sub-lines. Two of the cell lines, LAPC4 and MDA PCa 2b, mentioned earlier to have the most biological effect after DN FGFR treatment are also androgen sensitive prostate cancer cell lines. It might be interesting to test the effect of DN FGFR on different androgen sensitivity conditions.

For the examination of the effect of the DN FGFR on cell cycle progression, prostate cells were infected with AdDN FGFR and AdLacZ and flow cytometry analysis was performed after different time points (24, 48 and 72 hours). A summary of these results is shown in Figures 3 A and B.
All cell lines tested except C4-2 accumulated in G2/M 72 hours after the infection with DN FGFR. In 48 hours of infection with DN FGFR, C4-2 cells, however showed 20% increase in the number of cells in G2/M phase. The accumulation of cells in G2/M did not correlate the biological effect of DN FGFR in every cell line. For example, treatment of DN FGFR showed more biological effect on MDA PCa 2b cells as compared to 22Rv1 cells after 72 hours of infection (28% reduction in cell number after 72 hours of infection in 22Rv1 cells vs

A.

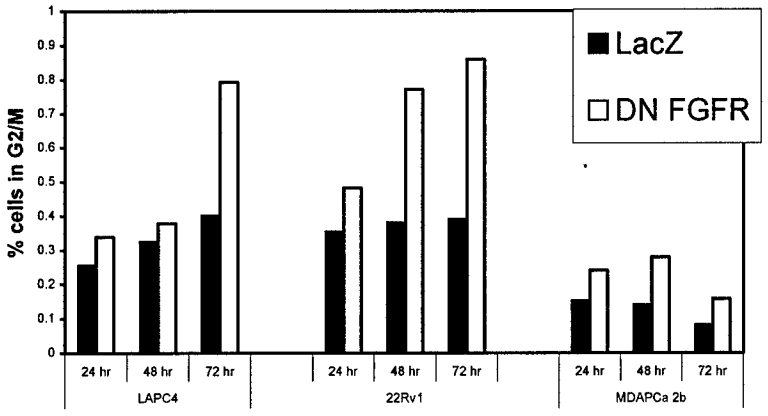

B.

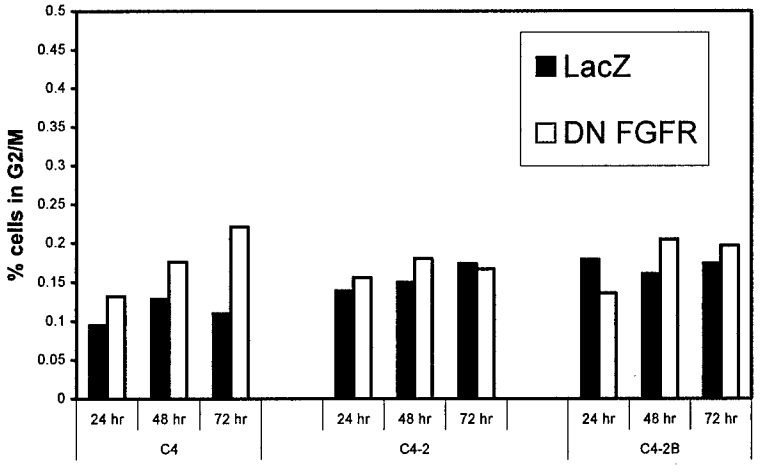

Figure 3. Prostate cancer cells, LAPC4, 22Rv1 and MDA Pca 2b (A) and C4, C4-2 and C-42B (B) were infected with AdDN FGFR and AdLacZ and flow cytometry analysis was performed after 24, 48 and 72 hours. Percent of the cells in G2 is shown in each on the y-axis.

68% reduction in MDA PCa 2b cells). However, The percentage of the cells in G2/M were 85 and 15 in 22 Rv1 and MDA PCa cells, respectively. This might require further investigation. 22 Rv1 cells might need more time to acquire the biological effect of DN FGFR. Cell cycle analysis of DN FGFR treated LAPC4 cells as a representation is shown in Figure 4.

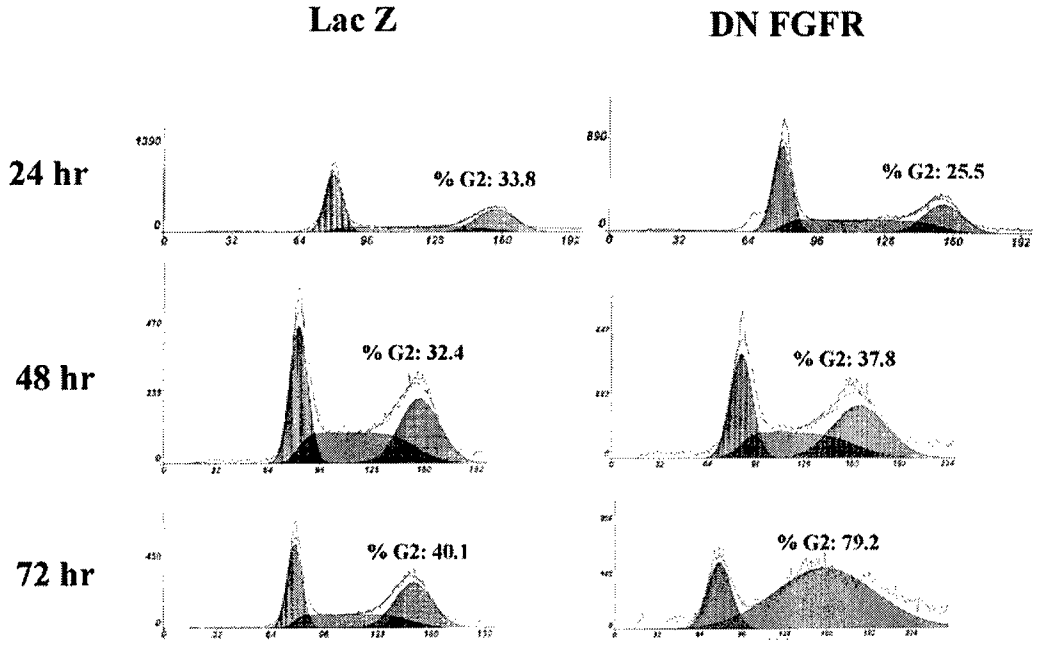

Figure 4. Cell cycle analysis of DN FGFR infected LAPC4 cells. In each case, cell number is represented on the y-axis, with the corresponding fluorescence at 550 nm is shown on the x-axis. Flow cytometry data are seen as a line, and filled area represents the result of cell cycle analysis by the use of Multi Cycle software. The percantage of G2/M as determined with this software is indicated.

Since the production of our original AdDN FGFR, further developments have been made in the area of adenoviral delivery to enhance the transduction ability of the vectors such as Ad5 and Ad35. The entry pathway for Ad5 consists of initial binding to the cell, which is mediated by the association of the Ad5 fiber protein and a 46-kd membrane protein called CAR, followed by internalization. CAR is a member of the immunoglobulin superfamily

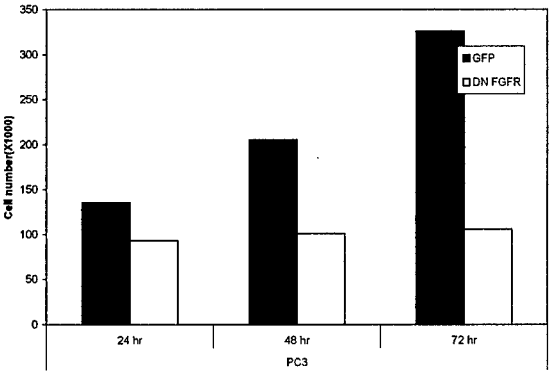

Figure 5. Effect of DN FGFR on cell proliferation and viability of PC3 prostate cancer cell line.

and also serves as the receptor for coxsackie B virus. Recently, a new adenovirus vector has been developed in which the fiber protein of adenovirus type 35 (Ad 35) has been substituted for the fiber protein of Ad5 that allows the virus to enter cells in a CAR-independent fashion. It has been shown that this new vector could efficiently transfer genes into hematopoietic stem cells and human bone marrow mesenchimal stem cells[Yotnda et al., 2001;Olmsted-Davis et al., 2002a;Shayakhmetov et al., 2000]. With the collaboration of our colleagues Drs. Elizabeth Olmsted-Davis and Alan Davis of Vector Development Core Facility at our Institution, we were able to construct Ad5F35 DN FGFR. This new adenovirus is highly efficient on affecting all the cell lines used. We were able to get efficient infection on PC3 cell line that has been failed to get infected with the previous adenovirus. Figure 5 shows the affect of the new adenovirus on PC3 cell proliferation.

Fortunately, we obtained a monoclonal antibody from Biodesign International, Inc. (Saco, ME) detecting extracellular domain of FGFR1. This antibody reacts with both alpha (denatured) and beta isoforms and the epitope is within the sequence his241 and val267 between Ig loops II and III. By using this antibody after titration for our experiments, we easily can show the successful infection of cells with AdDN FGFR. Figure 6 shows the detection of DN FGFR on Western blots. As seen in this figure DN FGFR infected PC3 cells showed a strong band, corresponding to DN FGFR protein, on a Western blot incubated with the new FGFR1 antibody, suggesting successful infection efficiency on PC3 cells after 24 hr time point. This data is verified in all cell lines used.

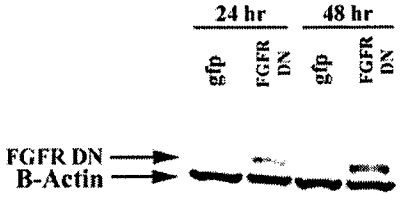

Figure 6. Detection of DN FGFR protein in AdDN FGFR treated cells.

Task 2: We proposed to investigate the growth inhibitory ability of DN FGFR in prostate cancer xenografts. Total of 35 Athymic NCr-nu/nu male homozygos 6-8 week-old nude mice were purchased from Charles Rivers Laboratory. Three way Differential Reactive Stroma (DRS) Xenograft tumors were generated as originally described by Tuxhorn et al.[Tuxhorn et al., 2002] 2 x106 LNCaP cells and 0.5X106 stromal cells were mixed with Matrigel and injected in each lateral flank of animal. Stromal cells were provided by Dr. David Rowley, from the department of Molecular and Cellular Biology of our Institution. Five animals (10 injection site) were used for each experiment set. A total of three sets for each of the DN FGFR and gfp infection are used. In one group when the tumor reached 0.5 mm in size AdDN FGFR is injected intratumorally. One animal was sacrificed after two rounds of injection to verify successful delivery of DN FGFR. The tumor lysed in lysis

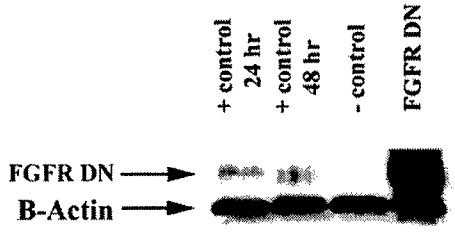

Figure 7. Detection of DN FGFR protein in AdDN FGFR treated xenografts.

buffer and the lysate subjected to Western blot experiments by using FGFR1 antibody described above. As seen in Figure 7, DN FGFR injected tumor showed remarkable expression of DN FGFR protein. We recently generated three way xenografts in one set of animals and waiting for the tumors to reach the appropriate size to start the viral injections. We are expecting to complete these in vivo experiments in next 2-3 months.

Task 3: In this task, we proposed to identify and cluster the differentially expressed genes in FGFR DN treated and untreated cells by microarray analysis across prostate cancer cell lines. In our preliminary experiments one of the differentially expressed genes in AdDN FGFR treated cells was CDC25C. CDC25 phosphatases belong to the tyrosine phosphatase family and play a critical role in regulating cell cycle progression by dephosphorylating cyclin dependent kinases at inhibitory residues. In human cells, cdc25 proteins are encoded by a multigene family, consisting of *CDC25A*, *CDC25B*, and *CDC25C[Hoffmann, 2000;Turowski et al., 2003].* In late G2, the *CDC25C* dephosphorylates Cdc2 on both threonine 14 and tyrosine 15, leading to the activation of Cdc2/cyclin B complexes[Graves et al., 2001;Dunphy and Kumagai, 1991;Strausfeld et al., 1991] and progression through the G2/M checkpoint. Phosphorylation of serine 216 of *CDC25C* throughout interphase and upon G2 checkpoint activation has been found to negatively regulate the enzymatic activity of *CDC25C* [Graves et al., 2000;Peng et al., 1997] and a positive feedback loop has been proposed between cdc2 and *CDC25C* [Hoffmann, 2000;Peng et al., 1997;Izumi and Maller, 1995;Strausfeld et al., 1991]. Activated Chk kinases can inactivate *CDC25C* via phosphorylation at serine 216, blocking the activation of cdc2 and transition into M-phase [Zeng et al., 1998]. Another aspect of Cdc25 regulation is alternative splicing that may produce at least five *CDC25B* variants [Baldin et al., 1997]. Splice variants are also reported for *CDC25A* and *C* [Wegener et al., 2000;Bureik et al., 2000]. The activity and regulation of *CDC25C* in prostate carcinoma has not been previously examined, despite its potentially important role in the G2/M transition in this common malignancy. To determine whether *CDC25C* plays a role in prostate cancer, we have examined the expression of *CDC25C* and its alternatively spliced variant in human prostate cancer. *CDC25C* protein is upregulated in comparison to normal prostate tissue and is present predominantly in its active dephosphorylated form. In addition, expression of a biologically active alternatively spliced *CDC25C* isoform is increased in prostate cancer. In addition, we have found, by expression of dominant negative fibroblast growth factor (FGF) receptors, that FGF signaling modulated *CDC25C* activity in prostate cancer, and in this manner can promote progression through the G2/M checkpoint.

This study on CDC25C was presented in tenth Annual Meeting of Association of Molecular Pathology and the abstract was published in the Journal of Molecular Diagnostics. The full length manuscript entitled "Increased expression and activity of CDC25C phosphatase and an alternatively spliced variant in prostate cancer" is in press in Clinical Cancer Research. Copies of accepted manuscript, published abstract and the letter of acceptance are attached.

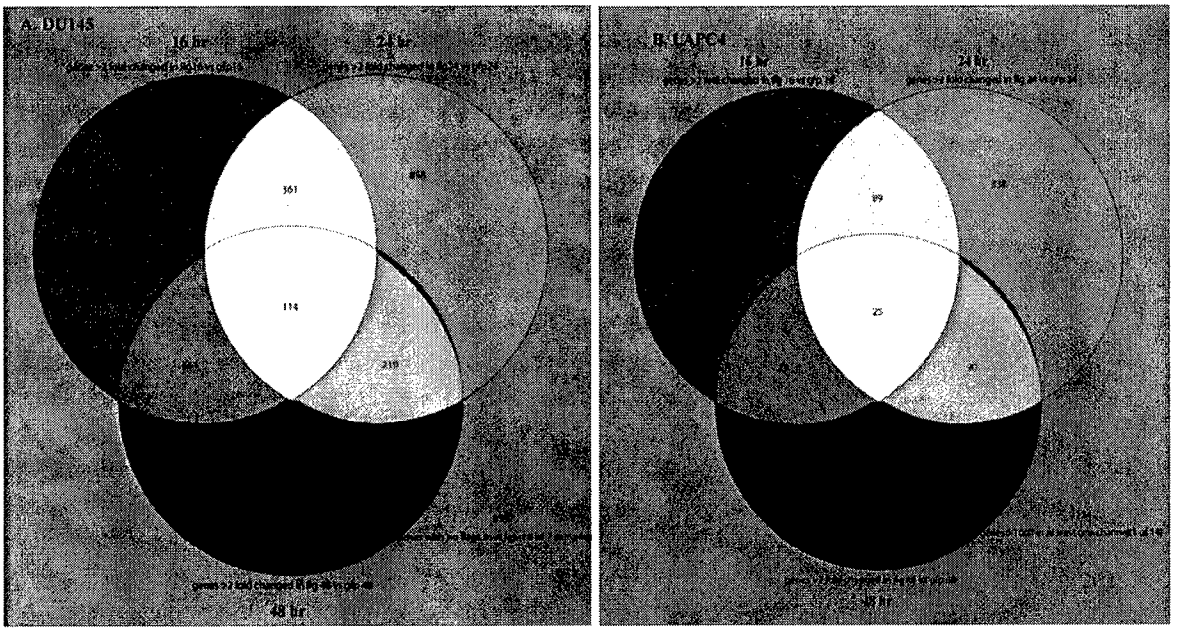

Figure 8. Summary of differentially expressed genes in DU145 (A) and LAPC4 (B) cell lines. The numbers of at least 2 fold differentially expressed genes are given inside the circles.

We have compared DU145 and LAPC4 cell lines treated with either gfp or DN FGFR carrying adenovirus in 16, 24, 48 and 72 hour time points. After hybridization and initial analysis, all data points were loaded to Gene Spring Software for further detail analysis. Microarray chip carrying oligonucleotides representing over 21 thousand human genes and transcripts obtained from Vancouver Microarray Core Facility (Vancouver, BC) were used. Data with low signal intensity, high background and high variability were eliminated. Array-specific data normalization was then performed using the LOWESS, "locally-weighted regression and smoothing scatter plots", procedure. Signals with raw intensity of less than 1000 in over half of the samples were also eliminated. The fold difference of the samples over the reference of these genes were calculated and grouped as they had over two fold differentially expressed values. Figure 8 shows the number of differentially expressed genes in DU145 cells in 8A and LAPC4 cells in 8B.

We have clustered these differentially expressed genes in all time points as seen in Figure 9. Gene annotations for these transcripts are given in Table 2.

A. DU145

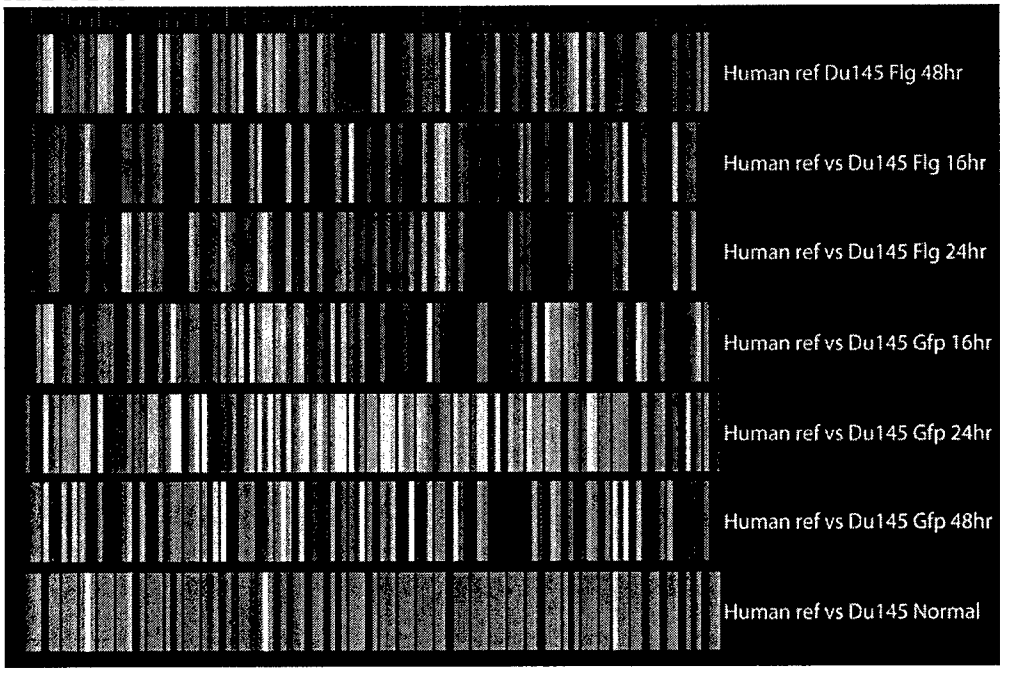

B. LAPC4

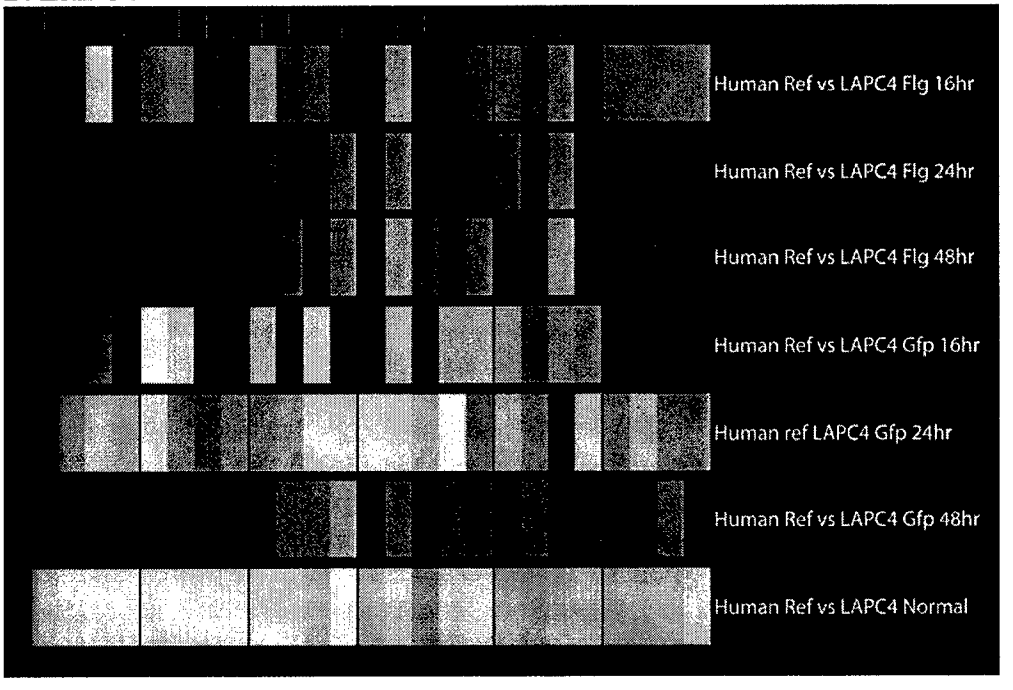

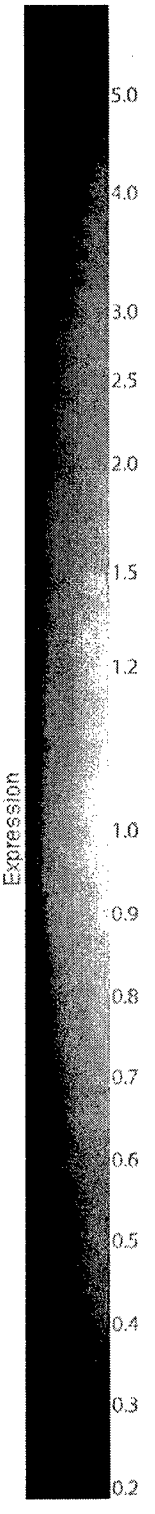

Figure 9. Clustering of the genes differentially expressed at least two folds at all time points in DU145 (A) and LAPC4 (B) cell lines. Each row represents a single sample and each column a single transcript. Each bar is colored by its expression at a given point as shown.

Table 2. Description of the genes differentially expressed in DU145 cells at all time points.

Fold change	Gene Description
12.76	Normal mucosa of esophagus specific 1^NMES1^NM_032413^112242^H2
7.523	Ras homolog gene family, member B^ARHB^NM_004040^204354^H200014
5.586	Homo sapiens cDNA FLJ14091 fis, clone MAMMA1000266^N/A^AK024153
5.378	Tyrosine 3-monooxygenase/tryptophan 5-monooxygenase activation
4.457	Homo sapiens cDNA FLJ25184 fis, clone CBR09423^N/A^AK057913^101
4.342	Homo sapiens cDNA FLJ14088 fis, clone MAMMA1000227^N/A^AK024150
4.239	Hypothetical protein FLJ10508^FLJ10508^NM_018118^274284^H200017
4.146	Likely homolog of mouse p140^KIAA1684^AB051471^278639^H20001733
4.104	PR domain containing 7^PRDM7^NM_052996^278234^H200017242
3.794	Homo sapiens, clone IMAGE:4851821, mRNA^N/A^BC015002^348705^H20
3.687	Centaurin, beta 1^CENTB1^NM_014716^108947^H200011613
3.498	Homo sapiens cDNA FLJ31060 fis, clone HSYRA2000925^N/A^AK055622
3.231	Homer, neuronal immediate early gene, 1B^SYN47^NM_004272^337737
3.191	Fibrillin3^KIAA1776^NM_032447^116265^H200012003
3.17	Homo sapiens cDNA FLJ11709 fis, clone HEMBA1005133^N/A^AK021771
3.15	Thyroid transcription factor 1^TITF1^U33749^197764^H200014771
2.99	Small inducible cytokine subfamily C, member 1 (lymphotactin)^S
2.982	Homo sapiens cDNA FLJ12209 fis, clone MAMMA1000962^N/A^AK022271
2.968	Homo sapiens mRNA full length insert cDNA clone EUROIMAGE 99418
2.819	Exonuclease 1^EXO1^NM_003686^47504^H200004844
2.815	Apolipoprotein M^G3A^NM_019101^247129^H200015859
2.814	ESTs, Moderately similar to located at OATL1 [H.sapiens]^N/A^BG
2.754	Putative UDP-GalNAc:polypeptide N-acetylgalactosaminyltransfera
2.736	Aryl hydrocarbon receptor nuclear translocator-like^ARNTL^NM_00
2.725	Hypothetical protein FLJ14494^FLJ14494^NM_032795^322406^H200018
2.689	Homo sapiens cDNA FLJ11599 fis, clone HEMBA1003879^N/A^AK021661
2.525	Homo sapiens putative ion channel protein CATSPER2 (CATSPER2),
2.505	Homo sapiens, clone IMAGE:4696946, mRNA, partial cds^N/A^BC0178
2.488	Homo sapiens mRNA; cDNA DKFZp586B0918 (from clone DKFZp586B0918
2.453	Lengsin^LGS^NM_016571^149585^H200013668
2.367	Hypothetical protein MGC20496^MGC20496^NM_052845^12106^H2000020
2.32	Carboxylesterase 2 (intestine, liver)^CES2^NM_003869^282975^H20
2.313	Ubiquitin-conjugating enzyme E2G 2 (UBC7 homolog, yeast)^UBE2G2
2.226	Homo sapiens mRNA full length insert cDNA clone EUROIMAGE 49248
2.209	ATP-dependent RNA helicase^ROK1^AK001652^99423^H200010964
2.179	Major histocompatibility complex, class I, F^HLA-F^NM_018950^11
2.169	Homo sapiens cDNA FLJ32921 fis, clone TESTI2006872^N/A^AK057483
2.164	Heterogeneous nuclear ribonucleoprotein H1 (H)^HNRPH1^NM_005520
2.157	Chemokine (C-X-C motif) ligand 16^CXCL16^NM_022059^82407^H20000
2.114	Homo sapiens cDNA FLJ31052 fis, clone HSYRA2000629, weakly simi
2.078	Hypothetical protein R33729_1^R33729_1^Z78330^10927^H200010095
2.049	KIAA1902 protein^KIAA1902^AB067489^7149^H200001372
2.007	Regulator of G-protein signalling 2, 24kD^RGS2^NM_002923^78944^
0.5	Interleukin 19^IL19^NM_013371^71979^H200005769
0.497	Hypothetical protein FLJ13593^FLJ13593^NM_024780^145807^H200013
0.497	Apolipoprotein L, 6^APOL6^NM_030641^257352^H200016431
0.494	CD37 antigen^CD37^NM_001774^153053^H200013851
0.491	Hypothetical protein FLJ21841^FLJ21841^NM_024609^29076^H2000038
0.487	Ribonuclease 6 precursor^RNASE6PL^AK001769^8297^H200001633
0.486	KIAA0770 protein^KIAA0770^BC015817^9452^H200001780
0.485	Retinoblastoma binding protein 5^RBBP5^NM_005057^72984^H2000058
0.473	Amplified in osteosarcoma^OS-9^AL137691^76228^H200006266
0.473	Rho GTPase activating protein 9^ARHGAP9^NM_032496^19807^H200002
0.466	Hypothetical protein FLJ10521^FLJ10521^NM_018125^116385^H200012

0.465	Homo sapiens cDNA FLJ30018 fis, clone 3NB692000529^N/A^AK054580
0.457	YDD19 protein^YDD19^U82319^350967^H200020967
0.449	Nuclear factor (erythroid-derived 2), 45kD^NFE2^NM_006163^75643
0.447	Low density lipoprotein receptor-related protein 4^LRP4^AB01154
0.444	DnaJ (Hsp40) homolog, subfamily C, member 3^DNAJC3^NM_006260^96
0.444	A disintegrin and metalloproteinase domain 11^ADAM11^NM_002390^
0.443	B7 protein^B7^NM_006992^155586^H200014095
0.442	Homo sapiens mRNA; cDNA DKFZp434G015 (from clone DKFZp434G015)^
0.438	Homo sapiens cDNA FLJ31499 fis, clone NT2NE2005441, weakly simi
0.432	Sprouty homolog 4 (Drosophila)^SPRY4^NM_030964^285814^H20000884
0.431	Kelch-like ECH-associated protein 1^KIAA0132^NM_012289^57729^H2
0.431	Receptor tyrosine kinase-like orphan receptor 2^ROR2^NM_004560^
0.43	Similar to RIKEN cDNA 1110002C08 gene^MGC9564^AK054669^343553^H
0.424	Homo sapiens mRNA for WNT14B, complete cds^N/A^NM_003396^350957
0.424	Kruppel-like factor 16^KLF16^NM_031918^303194^H200018168
0.41	Homo sapiens clone 23900 mRNA sequence^N/A^AF038184^293407^H200
0.406	Egf-like module containing, mucin-like, hormone receptor-like s
0.405	ESTs^N/A^AA278251^173345^H200014184
0.404	Homo sapiens cDNA: FLJ21572 fis, clone COL06651^N/A^AK025225^15
0.4	Matrix Gla protein^MGP^NM_000900^279009^H200017417
0.399	KIAA0610 protein^KIAA0610^AB011182^118087^H200012082
0.398	Homo sapiens cDNA FLJ25057 fis, clone CBL04590^N/A^AK057786^351
0.396	Hypothetical protein DKFZp762A227^DKFZp762A227^AL157431^274453^
0.395	Homeo box 11 (T-cell lymphoma 3-associated breakpoint)^HOX11^M6
0.388	Insulin-like growth factor 2 (somatomedin A)^IGF2^NM_000612^349
0.379	G protein-coupled receptor 23^GPR23^NM_005296^27812^H200003795
0.36	Protein tyrosine phosphatase, non-receptor type 7^PTPN7^NM_0028
0.359	Protein tyrosine phosphatase, receptor type, N polypeptide 2^PT
0.353	Tumor suppressing subtransferable candidate 4^TSSC4^NM_005706^1
0.353	Homo sapiens cDNA FLJ14130 fis, clone MAMMA1002618^N/A^AK024192
0.35	KIAA0825 protein^KIAA0825^AB020632^194755^H200014678
0.347	CGI-35 protein^LOC51077^NM_015962^343173^H200019907
0.338	Homo sapiens cDNA: FLJ21909 fis, clone HEP03834^N/A^AK025562^18
0.334	Hypothetical protein FLJ10477^FLJ10477^NM_018105^7432^H20000143
0.325	Sirtuin silent mating type information regulation 2 homolog 5 (
0.318	STE20-like kinase^JIK^AF181985^12040^H200002056
0.31	Cholecystokinin B receptor^CCKBR^NM_000731^203^H200000057
0.305	Homo sapiens cDNA FLJ25027 fis, clone CBL02392^N/A^AK057756^915
0.299	V-ets erythroblastosis virus E26 oncogene homolog 1 (avian)^ETS
0.295	Homo sapiens HSPC285 mRNA, partial cds^N/A^AF161403^293815^H200
0.285	Apelin; peptide ligand for APJ receptor^APELIN^NM_017413^303084
0.284	Homo sapiens mRNA; cDNA DKFZp586K1922 (from clone DKFZp586K1922
0.264	H2B histone family, member N^H2BFN^NM_003527^151506^H200013772
0.253	Homo sapiens cDNA FLJ30785 fis, clone FEBRA2000901^N/A^AK055347
0.25	H2A histone family, member K, pseudogene^H2AFKP^Z80777^334456^H
0.244	Short-chain alcohol dehydrogenase family member^HEP27^NM_005794
0.23	KIAA0211 gene product^KIAA0211^NM_014630^79347^H200006670
0.2	Homo sapiens clone CDABP0095 mRNA sequence^N/A^AY007155^46919^H
0.193	Carbamoyl-phosphate synthetase 1, mitochondrial^CPS1^NM_001875^
0.191	Follistatin^FST^NM_006350^9914^H200001854
0.174	BCL2-associated X protein^BAX^NM_004324^159428^H200007440
0.157	Homo sapiens mRNA full length insert cDNA clone EUROIMAGE 36278
0.154	Solute carrier family 18 (vesicular acetylcholine), member 3^SL
0.138	GATA binding protein 3^GATA3^NM_002051^169946^H200007883
0.126	Nuclear receptor binding protein^NRBP^NM_013392^272736^H2000169
0.0971	Protocadherin 1 (cadherin-like 1)^PCDH1^NM_032420^79769^H200006
0.0916	Homo sapiens mRNA; cDNA DKFZp564O0862 (from clone DKFZp564O0862
0.0912	Hypothetical protein FLJ20718^FLJ20718^NM_017939^50579^H2000049

Table 3. Description of the genes differentially expressed in LAPC4 cells at all time points. Only 24 hr time point fold change is shown.

Fold change	Gene Description
9.845	Hepatic leukemia factor^HLF^M95585^250692^H200016237
7.326	Annexin A5^ANXA5^NM_001154^300711^H200009920
2.539	WAS protein family, member 2^WASF2^NM_006990^347375^H200020128
2.462	Estrogen receptor binding site associated, antigen, 9^EBAG9^NM_
2.31	Putative 47 kDa protein^LOC56899^AF145204^92927^H200010556
2.162	Synaptogyrin 2^SYNGR2^NM_004710^5097^H200000996
0.495	Homo sapiens, Similar to RIKEN cDNA 0610030G03 gene, clone MGC:
0.489	Ras association (RalGDS/AF-6) domain family 1^RASSF1^NM_007182^
0.479	Glial cells missing homolog a (Drosophila)^GCMA^AB047819^28346^
0.423	Homo sapiens clone 24734 mRNA sequence^N/A^AF070625^12440^H2000
0.417	G protein-coupled receptor 35^GPR35^NM_005301^239891^H200015689
0.416	Homo sapiens, clone MGC:14381 IMAGE:4299817, mRNA, complete cds
0.375	KIAA0170 gene product^KIAA0170^NM_014641^277585^H200017229
0.371	KIAA0775 gene product^KIAA0775^NM_014726^94790^H200010662
0.37	Solute carrier family 20 (phosphate transporter), member 1^SLC2
0.327	Chromosome 14 open reading frame 4^C14orf4^AB058768^179260^H200
0.306	Homo sapiens mRNA; cDNA DKFZp564C142 (from clone DKFZp564C142)^ RAB3D, member RAS oncogene
0.291	family^RAB3D^NM_004283^251376^H20001
0.254	Homo sapiens cDNA FLJ13691 fis, clone PLACE2000100^N/A^AK023753
0.247	Protocadherin 1 (cadherin-like 1)^PCDH1^NM_032420^79769^H200006 Hypothetical protein
0.149	MGC4677^MGC4677^NM_052871^337986^H20001985
0.113	Annexin A2 pseudogene 1^ANXA2P1^M62896^348252^H200020164
0.0905	HLA-G histocompatibility antigen, class I, G^HLA-G^NM_002127^73
0.0388	Hypothetical protein FLJ23467^FLJ23467^NM_024575^16179^H2000025
0.0046	Acrosomal vesicle protein 1^ACRV1^NM_001612^169222^H200007794

We have synthesized cDNA from all the cell lines treated with either DN FGFR or GFP to use in Quantitative Real time RT-PCR analysis. Some of the interesting genes have been studied by this assay to verify their differential expression in DN FGFR treated cells. So far we have studied four genes including PCDH1, AKT3, AKT1 and ECT2. PCDH1 seemed to be interesting initially. However, after Quantitative Real time RT-PCR experiments, we did not see a consistent pattern of its expression in all DN FGFR treated cell lines. It would be more crucial for this study to find a candidate gene that plays an important role in FGFR signaling in all cell lines. Therefore, we did not proceed with this gene further.

As seen in Figure 10, the relative expression of AKT3 was significantly decreased 24 hr and 48 hr after treatment with DN FGFR in C4-2B cell line. LAPC4 cell line also showed similar pattern in earlier time points. More detail analysis of AKT3 and AKT1 in other cell lines in mRNA and protein levels is in progress. It will be significantly important if we can show that DN FGFR can disrupt the AKT pathway since this pathway is also involved in cell survival. We need more convincing data to make this conclusion and the experiments to elucidate this possibility are in progress.

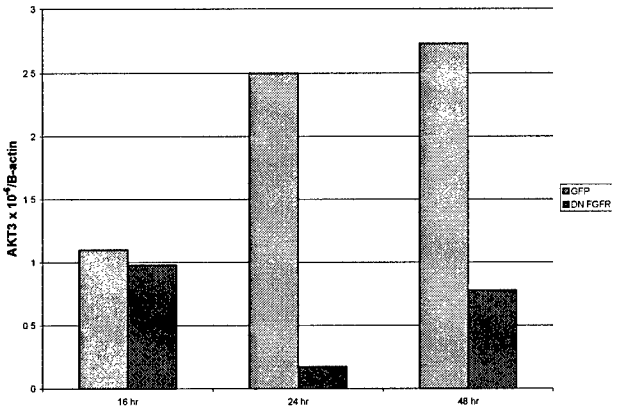

Figure 10. Relative expression of AKT3 in C4-2B cell line treated with gfp or DN FGFR.

The epithelial cell transforming gene 2 (ECT2) plays a critical role in cytokinesis and is phosphorylated in G2 and M phases of the cell cycle. It's drosophila homolog pbl has been shown to be induced by growth factors and FGF Receptor Heartless (HTL)[Schumacher et al., 2004;Saito et al., 2003]. Therefore, we thought to study this gene in our system. As shown in Figure 11, the expression of ECT2 was down-regulated in C4-2B cells in 16 and 48 hrs. We will extend this work to other cell lines as well. Additional microarray experiments and analysis are in progress to determine significant genes critical in FGFR signaling pathway.

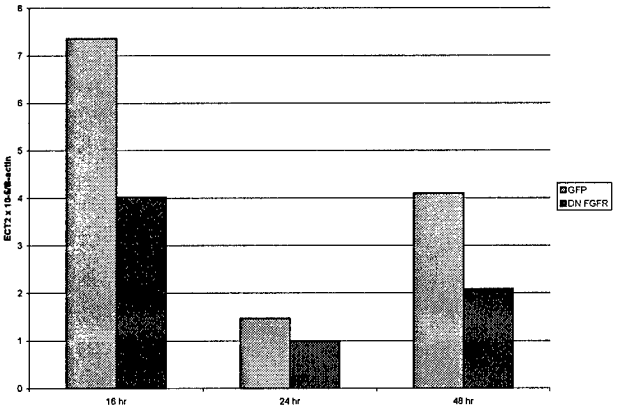

Figure 11. Relative expression of ECT2 in C4-2B cell line treated with gfp or DN FGFR.

Recently, Biosorce International, Inc., (Camarillo, CA), introduced a Mercator PhosphoArray Kit that is compatible with our Instruments. This is a protein

microarray detecting phosphorylation status of 10 proteins, including EGFR, FAK, Src, Paxillin, Akt, JNK1/2, p38, HSP27, ATF2 and CREB. These proteins are involved in different signaling pathways critical for cell migration, invasion and survival. We have done one preliminary experiment with this kit and obtained a promising data with p38 in DU145 cells treated with DN FGFR. P38 is involved in kinase activation loop and responds to stress signals. We will determine the activity of this protein in other cell lines we have. Since we already have set up the system and have the lysates, it should not take us long to complete these experiments. However, we understand that some of the data obtained from these experiments need to be verified in other systems and studied further which is beyond the scope of this project.

KEY RESEARCH ACCOMPLISHMENTS:

- Verification of DN FGFR effect on proliferation, survival and cell cycle of additional prostate cancer cell lines to determine FGF receptor signaling is essential for viability of human prostate cancer cells and disruption of this signaling via expression of a dominant negative FGF receptor-1 protein in human prostate cancer cells might contribute to the death of cancer cells.

- The G2/M transition may be a critical checkpoint in prostate cancer.

- Identification of increased CDC25C phosphatase activity and it's biologically active spliced form in prostate cancer and the role of fibroblast growth factor receptor signaling in its activity.

REPORTABLE OUTCOMES:

A published abstract: Ozen and Ittmann M: Increased CDC25C Phosphatase Activity in Prostate Cancer: Correlation to Biochemical Recurrence. Journal of Molecular Diagnostics 2004, (6)4: 431.

A manuscript in press: Ozen M and Ittmann M: Increased expression and activity of CDC25C phosphatase and an alternatively spliced variant in prostate cancer. Clinical Cancer research (in press).

CONCLUSIONS:

A research in this report supports that FGF receptor signaling is essential for viability of human prostate cancer cells and disruption of this signaling via expression of a dominant negative FGF receptor-1 protein in human prostate cancer cells might contribute to the death of cancer cells. These findings reveal that prostate cancer cells treated with DN FGFR is arrested G2/M phase of cell cycle and eventually die. FGF signaling modulated *CDC25C* activity in prostate cancer, and in this manner can promote progression through the G2/M checkpoint. *CDC25C* protein is upregulated in comparison to normal prostate tissue and is present almost exclusively in its active dephosphorylated

form. Expression of a biologically active alternatively spliced *CDC25C* isoform is also increased in prostate cancer. A better understanding of the mechanism by which FGF signaling is regulated and determining other molecules involved in this pathway contributing tumor growth and survival will facilitate the development of cancer therapies to target FGF signaling pathway.

REFERENCES:

Baldin V, Cans C, SupertiFurga G, Ducommun B (1997) Alternative splicing of the human CDC25B tyrosine phosphatase. Possible implications for growth control? *Oncogene* 14: 2485-2495

Bureik M, Rief N, Drescher R, Jungbluth A, Montenarh M, Wagner P (2000) An additional transcript of the cdc25C gene from A431 cells encodes a functional protein. *International Journal of Oncology* 17: 1251-1258

Craft N, Shostak Y, Carey M, Sawyers CL (1999) A mechanism for hormone-independent prostate cancer through modulation of androgen receptor signaling by the HER-2/neu tyrosine kinase. *Nature Medicine* 5: 280-285

Dunphy WG, Kumagai A (1991) The Cdc25 Protein Contains An Intrinsic Phosphatase-Activity. *Cell* 67: 189-196

Giri D, Ropiquet F, Ittmann M (1999) Alterations in expression of basic fibroblast growth factor (FGF) 2 and its receptor FGFR-1 in human prostate cancer. *Clinical Cancer Research* 5: 1063-1071

Graves PR, Lovly CM, Uy GL, Piwnica-Worms H (2001) Localization of human Cdc25C is regulated both by nuclear export and 14-3-3 protein binding. *Oncogene* 20: 1839-1851

Graves PR, Yu LJ, Schwarz JK, Gales J, Sausville EA, O'Connor PM, Piwnica-Worms H (2000) The Chk1 protein kinase and the Cdc25C regulatory pathways are targets of the anticancer agent UCN-01. *Journal of Biological Chemistry* 275: 5600-5605

Green AP, Huang JJ, Scott MO, Kierstead TD, Beaupre I, Gao GP, Wilson JM (2002) A new scalable method for the purification of recombinant adenovirus vectors. *Human Gene Therapy* 13: 1921-1934

Hoffmann I (2000) The role of Cdc25 phosphatases in cell cycle checkpoints. *Protoplasma* 211: 8-11

Izumi T, Maller JL (1995) Phosphorylation and Activation of the Xenopus Cdc25 Phosphatase in the Absence of Cdc2 and Cdk2 Kinase-Activity. *Molecular Biology of the Cell* 6: 215-226

Navone NM, Olive M, Ozen M, Davis R, Troncoso P, Tu SM, Johnston D, Pollack A, Pathak S, von Eschenbach AC, Logothetis CJ (1997) Establishment of two human prostate cancer cell lines derived from a single bone metastasis. *Clinical Cancer Research* 3: 2493-2500

Olmsted-Davis EA, Gugala Z, Gannon FH, Yotnda P, McAlhany RE, Lindsey RW, Davis AR (2002a) Use of a chimeric adenovirus vector enhances BMP2 production and bone formation. *Human Gene Therapy* 13: 1337-1347

Olmsted-Davis EA, Gugala Z, Gannon FH, Yotnda P, McAlhany RE, Lindsey RW, Davis AR (2002b) Use of a chimeric adenovirus vector enhances BMP2 production and bone formation. *Human Gene Therapy* 13: 1337-1347

Ozen M, Giri D, Ropiquet F, Mansukhani A, Ittmann M (2001) Role of fibroblast growth factor receptor signaling in prostate cancer cell survival. *Journal of the National Cancer Institute* 93: 1783-1790

Peng CY, Graves PR, Thoma RS, Wu ZQ, Shaw AS, PiwnicaWorms H (1997) Mitotic and G(2) checkpoint control: Regulation of 14-3-3 protein binding by phosphorylation of Cdc25C on serine-216. *Science* 277: 1501-1505

Polnaszek N, Kwabi-Addo B, Peterson LE, Ozen M, Greenberg NM, Ortega S, Basilico C, Ittmann M (2003) Fibroblast growth factor 2 promotes tumor progression in an autochthonous mouse model of prostate cancer. *Cancer Research* 63: 5754-5760

Saito S, Tatsumoto T, Lorenzi MV, Chedid M, Kapoor V, Sakata H, Rubin J, Miki T (2003) Rho exchange factor ECT2 is induced by growth factors and regulates cytokinesis through the N-terminal cell cycle regulator-related domains. *J Cell Biochem* 90: 819-836

Schumacher S, Gryzik T, Tannebaum S, Muller HA (2004) The RhoGEF Pebble is required for cell shape changes during cell migration triggered by the Drosophila FGF receptor Heartless. *Development* 131: 2631-2640

Shayakhmetov DM, Papayannopoulou T, Stamatoyannopoulos G, Lieber A (2000) Efficient gene transfer into human CD34(+) cells by a retargeted adenovirus vector. *Journal of Virology* 74: 2567-2583

Sramkoski RM, Pretlow TG, Giaconia JM, Pretlow TP, Schwartz S, Sy MS, Marengo SR, Rhim JS, Zhang DS, Jacobberger JW (1999) A new human prostate carcinoma cell line, 22R upsilon 1. *In Vitro Cellular & Developmental Biology-Animal* 35: 403-409

Strausfeld U, Labbe JC, Fesquet D, Cavadore JC, Picard A, Sadhu K, Russell P, Doree M (1991) Dephosphorylation and Activation of A P34Cdc2 Cyclin-B Complex Invitro by Human Cdc25 Protein. *Nature* 351: 242-245

Takahashi, H. Studies on the expression of fibroblast growth factors and fibroblast growth factor receptors in human prostate cancer. Nippon Hinyokika Gakkai Zasshi 89, 836-845. 1998.

Thalmann GN, Sikes RA, Wu TT, Degeorges A, Chang SM, Ozen M, Pathak S, Chung LW (2000) LNCaP progression model of human prostate cancer: androgen-independence and osseous metastasis. *Prostate* 44: 91-103

Turowski P, Franckhauser C, Morris MC, Vaglio P, Fernandez A, Lamb NJC (2003) Functional cdc25C dual-specificity phosphatase is required for S-phase entry in human cells. *Molecular Biology of the Cell* 14: 2984-2998

Tuxhorn JA, McAlhany SJ, Yang F, Dang TD, Rowley DR (2002) Inhibition of transforming growth factor-beta activity decreases angiogenesis in a human prostate cancer-reactive stroma xenograft model. *Cancer Res* 62: 6021-6025

Wegener S, Hampe W, Herrmann D, Schaller HC (2000) Alternative splicing in the regulatory region of the human phosphatases CDC25A and CDC25C. *European Journal of Cell Biology* 79: 810-815

Yotnda P, Onishi H, Heslop HE, Chen D, Chiu W, Piedra PA, Takahashi S, Barry M, Davis A, Templeton NS, Brenner MK (2002) Targeting adenovectors to hemopoietic cells. *Blood Cells Molecules and Diseases* 28: 347

Yotnda P, Onishi H, Heslop HE, Shayakhmetov D, Lieber A, Brenner M, Davis A (2001) Efficient infection of primitive hematopoietic stem cells by modified adenovirus. *Gene Therapy* 8: 930-937

Zeng Y, Forbes KC, Wu ZQ, Moreno S, Piwnica-Worms H, Enoch T (1998) Replication checkpoint requires phosphorylation of the phosphatase Cdc25 by Cds1 or Chk1. *Nature* 395: 507-510

APPENDICES:

A manuscript by Ozen M and Ittmann M: Increased CDC25C phosphatase activity in prostate cancer: role of fibroblast growth factor receptor signaling. Clinical Cancer Research (in press).

Acceptance letter for the above manuscript

An abstract published in the Journal of Molecular Diagnostics.

Increased expression and activity of CDC25C phosphatase and an alternatively spliced variant in prostate cancer.

Mustafa Ozen and Michael Ittmann

Department of Pathology, Baylor College of Medicine and Michael E. DeBakey Dept. of Veterans Affairs Medical Center, Houston, Texas 77030

Running Title: CDC25C activity is increased in prostate cancer

Key Words: CDC25C, alternative splicing, prostate cancer, Ki-67, proliferation

Abbreviations: polymerase chain reaction (PCR); prostate specific antigen (PSA), benign prostatic hyperplasia (BPH)

Correspondence:

Michael Ittmann MD/PhD
Research Service
Michael E. DeBakey VAMC
2002 Holcombe Blvd
Houston, TX 77030
Tele: (713) 791-1414 X4008
Fax : (713) 794-7938
E-mail: mittmann@bcm.tmc.edu

ABSTRACT

Alterations in the control of cell cycle progression have been implicated in a wide variety of malignant neoplasms, including prostate cancer. CDC25 phosphatases belong to the tyrosine phosphatase family and play a critical role in regulating cell cycle progression by dephosphorylating cyclin dependent kinases at inhibitory residues. CDC25C plays an important role in the G2/M transition by activating Cdc2/Cyclin B1 complexes. To determine whether CDC25C activity is altered in prostate cancer, we have examined the expression of CDC25C and an alternatively spliced variant in human prostate cancer samples and cell lines. CDC25C protein is upregulated in prostate cancer in comparison to normal prostate tissue and is present almost exclusively in its active dephosphorylated form. Expression of a biologically active alternatively spliced CDC25C isoform is also increased in prostate cancer and expression of alternatively spliced CDC25C is correlated to occurrence of biochemical (PSA) recurrence. We have also developed a quantitative RT-PCR analysis of Ki-67 expression as a method of measuring proliferative activity in prostate cancer from RNA samples. Based on this analysis of Ki-67 expression, some, but not all of this increase in CDC25C and its alternatively spliced variants is correlated with increased proliferation in prostate cancer. This data suggests that CDC25C might play an important role in prostate cancer progression and could be used to monitor and predict the aggressiveness of this disease.

INTRODUCTION

Abnormal expression and/or activity of cell cycle regulatory proteins have been identified in a wide variety of malignant neoplasms, including prostate cancer. Cell cycle progression is controlled by the sequentially activities of cyclin dependent kinases, whose activities are tightly regulated by cyclins, cyclin dependent kinase inhibitors and a variety of other proteins. Several groups have shown increased expression of cyclin B1, which plays a critical role in the G2/M transition, in human prostate cancers (1,2). Recent work by Maddison et al.(3) has demonstrated increased levels of cyclin B1 in poorly differentiated and androgen independent prostate cancers in the TRAMP mouse model of prostate cancer. During G2, the Cdc2/Cyclin B complex is kept inactive by phosphorylation of Cdc2 by Wee1. At the onset of mitosis, Cdc2/Cyclin B complexes are dephosphorylated by CDC25 phosphatase leading to increased kinase activity (4-6). Our laboratory has demonstrated previously that disruption of fibroblast growth factor signaling in prostate cancer cells leads to decrease in Cdc2 kinase activity and arrest in G2, followed by cell death (7). These findings imply that the G2/M transition may be a critical checkpoint in prostate cancer.

CDC25 phosphatases belong to the tyrosine phosphatase family and play a critical role in regulating cell cycle progression by dephosphorylating cyclin dependent kinases at inhibitory residues. In human cells, CDC25 proteins are encoded by a multigene family, consisting of *CDC25A*, *CDC25B*, and *CDC25C* (8). In late G2, CDC25C dephosphorylates Cdc2 on both threonine 14 and tyrosine 15, leading to the activation of Cdc2/Cyclin B complexes (9-11) and progression through the G2/M checkpoint. Phosphorylation of serine 216 of CDC25C throughout interphase and upon G2

checkpoint activation has been found to negatively regulate the activity of CDC25C by cytoplamic sequestration (12,13) and a positive feedback loop has been proposed between Cdc2 and CDC25C (11,13-15). Activated Chk kinases can phosphorylate CDC25C at serine 216, blocking the activation of Cdc2 and transition into M-phase (16). Another aspect of CDC25 regulation is alternative splicing that may produce at least five CDC25B variants (17), and splice variants are also reported for CDC25A and CDC25C (18,19). The activity and regulation of CDC25C in prostate carcinoma has not been previously examined, despite its potentially important role in the G2/M transition in this common malignancy.

To determine whether CDC25C plays a role in prostate cancer, we have examined the expression of CDC25C and an alternatively spliced variant in human prostate cancer samples and cell lines at both the protein and RNA levels. CDC25C protein is upregulated in comparison to normal prostate tissue and is present predominantly in its active dephosphorylated form. At the transcriptional level, CDC25C and an alternatively spliced variants were both overexpressed in prostate cancer. The expression of the spliced variants were correlated with biochemical recurrence.

MATERIALS AND METHODS

Tissue acquisition and extraction: Normal peripheral zone, hyperplastic transition zone (BPH) and cancer tissues were collected from men undergoing radical prostatectomy for clinically localized prostate cancer by Baylor prostate cancer SPORE Tissue Core and snap frozen. Benign tissues were confirmed to be free of cancer and cancer tissues contained at least 70% carcinoma. RNAs were extracted from 17 normal peripheral zone tissues, 7 BPH tissues and 58 prostate cancers using TRIzoL Reagent (Invitrogen, Carlsbad, CA) as described in the manufacturer's protocol. We analyzed 20 cancers with no evidence of prostate specific antigen (PSA) recurrence after 5 years of follow-up, 19 cancers with delayed PSA recurrence (mean time to recurrence 34.1 months) and 19 cancers with early recurrence i.e. less than one year (mean time to recurrence 4.5 months). PSA recurrence was defined as serum PSA greater than 0.2 ng/ml. Protein extracts were prepared as described previously (20) from 10 cancers and 8 normal peripheral zone tissues.

Reverse transcriptase-PCR and agarose gel elecrophoreisis: RNAs extracted from the prostate tissues were first reverse transcribed as previously described (21) and analyzed for the presence of two different cDNAs for CDC25C using the following primers flanking the deletions of the CDC25C sequence: forward, 5'-AGA GAG AAG CTT ATG TCT ACG GAA CTC TTC TCA TCC-3'; reverse, 5'-CCC AAA TAT TTC ATT TCA CTG TCC-3' as described previously by Bureik et al. (19). The β-actin primers were as described previously (22). Thirty-five cycles with the following program were performed: denaturation at 94°C for 1 min, annealing at 60°C for 1.5 min, elongation at 72°C for 1 min followed by 5 min extension at 72°C. The reaction was performed with

the Takara kit (Takara Bio, Inc, Japan) following the manufacturer's protocol. The PCR products were analyzed on a 1.5 % agarose gels and stained with ethidium bromide.

Cell lines: DU145, PC3 and LNCaP human prostate cancer cell lines were cultured in RPMI-1640 medium supplemented with 1% antibiotic and antimycotic (Gibco, Invitrogen, Carlsbad, CA) and 10% fetal bovine serum (FBS).

Quantitative real-time PCR and Primer Design. Real-time RT-PCR was carried out in iCycler real-time thermal cycler (BioRad, Hercules, CA) as described previously (22), incorporating the optimized PCR reaction conditions for each primer set. Oligonucleotide primers for CDC25C were carefully designed to cross exon/intron regions and to avoid self complementarity or the formation of primer-dimers and hairpins. Two primer sets, one detecting only the full length CDC25C by binding in the region deleted in the alternatively spliced variant (forward 5'-GCCACTCAGCTTACCACTTC-3'; reverse 5'-ATTTCATTTCACTGTCCACCAAG-3'), and the other detecting both spliced variant and the full length CDC25C (forward 5'-GACACCCAGAAGAGAATAATCATC-3'; reverse 5'-CGACACCTCAGCAACTCAG-3') were used. Alternatively spliced transcript levels were calculated by subtraction of full-length CDC25C transcript levels from the total CDC25C levels. This approach allows quantitation of the major alternatively spliced isoforms detected in prostate cancer cells, specifically the C5 and C4 variants described by Wegener et al. (18). The primers for Ki67 were as follows: forward, 5'-ACGAGACGCCTGGTTACTA TC-3'; reverse, 5' –GCTCATCAATAACAGACC CATTTAC-3'. The β-actin primers were as described previously (22). The threshold cycle (Ct) values in log linear range representing the detection threshold values was used

for quantitation and expressed as copy numbers based on a standard curve generated using plasmid DNA.

***Western blot analysis*:** The tissue samples were homogenized and lysed in lysis buffer (20) and cleared by centrifugation for 10 min in a microcentrifuge at 4°C. Protein concentration was determined using a BioRad protein assay. The lysates were then boiled in sample buffer, centrifuged and the 30 ug of supernatant protein subjected to sodium dodecyl sulfate-polyacrylamide (SDS-PAGE) electrophoresis using a 10% gel. The resolved proteins were electrotransferred to nitrocellulose membranes and then blocked with phosphate buffered saline with 0.5% Tween 20 (PBST) containing 5% fat-free milk. Western blot for CDC25C was performed using 500 ng/ml polyclonal anti-CDC25C antibody (C20, Santa Cruz Biotechnology, Santa Cruz, CA) and anti-phosphoCDC25C (ser 216) antibody (901, Cell Signaling Technology, Beverly, MA) at 4^0 for 16 hrs. The membranes then were washed with PBST and treated with appropriate secondary antibody. The antigen-antibody reaction was visualized using an enhanced chemiluminescence (ECL) assay (Amersham, Arlington Hts, IL) and exposure to ECL film (Amersham). Control antibody was an anti-β-actin monoclonal antibody (A5316, Sigma) used at a 1:5000 dilution. To determine the specificity of the bands observed in Western blots for CDC25, anti-CDC25C antibody was pre-incubated with five fold molar excess of the blocking peptide (sc-327 P, Santa Cruz Biotechnology) for 2 hr at room temperature before use in the Western blot protocol. For quantitative Western blotting studies, the intensities of the bands on the Western blots were quantified as densitometric units (DU) by using the GelExpert software package supplied with the Nucleovision gel imaging system (Nucleo Tech Corporation, Hayward, CA).

RESULTS

Activity of CDC25C protein in clinically localized human prostate cancers.

To evaluate the *in vivo* activity of CDC25C in prostate cancer tissues, we determined the levels of total and phosphorylated CDC25C protein in the lysates from normal prostate peripheral zone and prostate cancer tissue samples. Out of 9 evaluable cancer samples, only two had readily detectable amounts of phospho-CDC25C (Fig. 1). In contrast, in the same blots normal prostate peripheral zone samples had detectable phospho-CDC25C protein in 6 of 8 samples. Total CDC25C protein was detectable in 6 of 9 cancer cases whereas only 2 of 8 normal tissue samples showed detectable total CDC25C when analyzed in the same blots (Fig. 1). Thus, in cancer tissues there is both markedly increased CDC25C protein and much less of its inactive phosphorylated form.

Alternatively spliced CDC25C variant is detected in prostate cancer RNA and in prostate cancer cell lines.

In addition to the full length CDC25C protein examined above, there are alternatively spliced of CDC25C transcripts that have been detected in a number of cancer cell lines (18,19). The immunoglobin heavy chain, that is present in large amounts in some patient samples, may interfere with direct measurement of the alternatively spliced proteins in clinical samples. We therefore analyzed RNAs from prostate cancer cell lines and a second set of clinically localized prostate cancers for the presence of the CDC25C alternatively spliced variants using RT-PCR and electrophoreisis on agarose gels (Figure 2A). The full length wild type (WT) and alternatively spliced CDC25C transcripts are present in both LNCaP and DU145 prostate cancer cell lines (Fig. 2A). The major alternatively spliced isoform corresponds to the C5 variant described by Wegener et al.

(18). Other variant transcripts, intermediate in size between the WT and C5 transcripts were present in lower amounts as well. The C5 CDC25C transcript was detectable by this methodology in 29 of 58 prostate cancer RNAs. In contrast, only 3 of 17 normal peripheral zone samples and none of the seven BPH samples had detectable quantities of this variant. The difference between the cancer and benign samples was statistically significant ($p=0.002$, Fisher exact test). In addition, the presence of the variant was strongly associated with the occurrence of biochemical (PSA) recurrence. Overall, the variant was present in cancer samples from 23 of 38 patients with biochemical recurrence but only 6 of 20 without PSA recurrence. This difference was statistically significant ($p=0.027$, Pearson's chi square). Since PSA recurrence, particularly early PSA recurrence, is associated with aggressive disease and decreased patient survival, this observation implies that expression of the variant mRNA is higher in aggressive prostate cancers. No statistically significant correlation of expression of the CDC25C variant with preoperative PSA or pathological stage was detected. As illustrated in Figure 2A, the cancer tissues also appeared to express increased amounts of WT mRNA in addition to expressing the variant mRNA, consistent with our observation of increased levels of WT CDC25C protein in the prostate cancer extracts.

We studied the presence of alternatively spliced CDC25C variant protein in prostate cancer cell lines to confirm its expression at the protein level (Figure 2B). Both the WT and C5 variant are expressed in all three of the commonly used prostate cancer cell lines (DU145, LNCaP and PC3). The specificity of the antibody for the WT and C5 variant was confirmed by pre-incubation of the anti-CDC25C antibody with excess peptide immunogen, which abolished both bands in a Western blot of LNCaP cell extract.

Other variant CDC25C proteins are also present in lower amounts, particularly in PC3 cells. To determine if the C5 variant is phosphorylated at the serine 216 residue, which is associated with cytoplasmic sequestration and loss of biological activity, we analyzed Western blots of DU145 protein extracts with a serine 216 specific anti-phospho-CDC25C antibody. No phosphorylation at serine 216 was detected in the C5 variant despite the readily detectable phosphorylation of the WT protein.

To assess the relationship between the level of WT and spliced variant proteins and mRNA levels we carried out quantitative RT-PCR to detect WT or spliced variant mRNAs and performed Western blots with serial dilutions of protein extracts from the same cells with anti-CDC25C antibody. We used both actively proliferating and confluent DU145 cells in these studies. As described in Materials and Methods, the quantitative RT-PCR assay used measures both the C4 and C5 mRNA variants (and potentially other variants) as alternatively spliced transcripts, although based on the gel electrophoreisis in Figure 2A, the C5 variant appears to be the dominant form. Western blots were scanned to quantitatively determine the band intensity of WT and alternatively spliced isoforms and the ratio of protein band intensity (as densitometric units) per ug protein to RNA copy number determined. For actively growing cells this ratio was 11.1 X 10^{-3} for WT Vs 2.21 X 10^{-3} for the spliced variant and for confluent cells this ratio was 2.8 X 10^{-3} for WT Vs 0.94 X 10^{-3}. Thus the WT transcript is associated with approximately 3-5 times more protein per transcript when compared to the alternative spliced transcript. Whether this is due to differences in translation efficiency or protein stability (or both) is not known.

To confirm our qualitative observations in the clinical with more rigorous quantitative data, we determined the expression levels of CDC25C WT and the spliced variants by real-time RT-PCR assay. Quantitative analysis of expression of WT CDC25C mRNA revealed a four fold increase in WT mRNA in cancer tissues relative to normal tissues (0.3 +/- .08 CDC25C transcripts/ 10^4 β-actin transcripts in normal Vs 1.28 +/- 0.2 CDC25C transcripts/ 10^4 β-actin transcripts in cancer tissues; mean +/- SEM). This difference was statistically significant ($P<0.001$, Mann Whitney Rank Sum test). In addition, as can be seen in Figure 3, there is a statistically significant increase in the expression of both total CDC25C and CDC25C splice variant mRNA in recurrent prostate cancers ($p=0.037$ and $p<0.001$, respectively, Mann Whitney) when compared to non-recurrent cancers. This increase is particularly marked in the prostate cancers with early recurrence. It should be noted that although the amount of spliced variant mRNAs in the recurrent cancers is about equal to the amount of WT mRNA, the amount of spliced variant protein(s) is probably three to five fold lower, based on the quantitative studies in DU145 cells described above.

Determination of Ki-67 RNA levels by real time quantitative RT-PCR as measurement for proliferative activity and normalization of CDC25C levels.

Since CDC25 is involved in control of exit from the G2 phase of the cell cycle, it is likely that the differences between normal and cancer tissues and non-recurrent and recurrent cancer tissues may be associated with differences in proliferative activity. To address this question, we designed a real time RT-PCR assay to determine RNA levels of the proliferation marker, Ki-67. The monoclonal antibody recognizing Ki-67 is routinely used in oncology to assess the proliferative index of tumor cells. Ki-67 transcript levels

were approximately two fold higher in the cancer tissues when compared to normal peripheral zone tissues ($p=0.001$, Mann-Whitney). As seen in Figure 4, relative expression of Ki-67 to β-actin was increased in Gleason Score 7-9 cases (Vs Gleason scores 5-6) and in cases with extracapsular extension and seminal vesicle invasion (Vs organ confined cancers), although not in cases with lymph node metastasis (Fig. 4). Ki-67 mRNA was also increased in prostate cancers that recurred (Vs non-recurrent cancers), particularly the cancers with early PSA recurrence (Fig. 4). The difference between the Ki-67 transcript levels in non-recurrent versus those with early recurrence was statistically significant ($p=0.032$, Mann Whitney). Overall, as expected, increased Ki-67 transcript levels were associated with pathological and clinical parameters indicative of aggressive disease.

We then examined the correlation between CDC25C and Ki-67 transcript levels using the Pearson Product Moment test. There was a statistically significant correlation between the Ki-67 transcript levels and total, WT and variant CDC25C transcript levels ($p<0.001$, $p<0.001$, $p<0.018$, respectively). The correlation coefficients ranged from 0.5-0.6, implying that a substantial fraction, but not all, of the variance in CDC25C levels is associated with differences in proliferation. As an alternative way to examine this association, we normalized expression of CDC25C expression levels using Ki-67 transcript levels determined on the same cDNAs rather than β-actin levels (Figure 5). Using this normalization, expression levels of the CDC25C splice variants was still significantly increased in patients with subsequent biochemical recurrence, including patients with either early ($p=0.041$) and late recurrence ($p=0.044$). The level of the Ki-67 normalized alternatively spliced CDC25c mRNA was also significantly higher in cancers

with higher Gleason score (Gleason 7-9 Vs 5-6; p=0.044, Mann Whitney) and was higher in cases with extracapsular extension, seminal vesicle invasion and lymph node metastasis, although these differences were not statistically significant.

DISCUSSION

CDC25A and CDC25B have been shown to collaborate with either mutation in the RAS oncogene or loss of retinoblastoma protein in transformation and, in this initial report, CDC25B protein was increased in 32% of human breast cancers (23). Subsequently, increased expression of CDC25A has been demonstrated in head and neck(24), non-small cell lung(25), gastric (26) and colon cancers(27) while CDC25B is increased in non-Hodgkin's lymphomas(28), as well as head and neck(24), non-small cell lung(25), gastric(26), colon(27), pancreatic(28) and prostate cancers (29). In contrast, increased expression of CDC25C has only been reported in a fraction of colon (27) and endometrial cancers(30). We have shown that the majority of prostate cancers have both increased total WT CDC25C protein and less phosphorylated CDC25C when compared to normal prostatic tissue. The level of WT CDC25C mRNA was increased 4-fold in cancer tissues consistent with these increased protein levels. Thus there are significantly higher levels of WT CDC25C protein in prostate cancer and much less of its inactive phosphorylated form, consistent with a marked increase in CDC25C phosphatase activity in prostate cancer.

In addition to the full length CDC25C mRNA, we detected a major alternatively spliced CDC25C in both human prostate cancers *in vivo* and in prostate cancer cell lines. This alternatively spliced transcript has a deletion of exons 3, 5 and 6 of the CDC25C gene and encodes a smaller protein containing the carboxy terminal catalytic domain and

17 unique amino acids. This alternatively spliced variant can complement a *CDC25C* mutant strain of *S. Pombe* (19). It is interesting to note that this variant leads to an increased uncoupling of the onset of mitosis and the completion of DNA synthesis in this mutant strain of *S. Pombe*, implying poor regulation of the activity of this variant protein. This alternatively spliced RNA was detected as visible band in one half of the prostate cancers analyzed but in only 16% of the benign tissues. The presence of this variant was significantly correlated with biochemical (PSA) recurrence following radical prostatectomy. Quantitative RT-PCR studies confirmed a significant increase in variant CDC25C mRNAs in prostate cancer and its correlation with PSA recurrence, particularly early PSA recurrence which is associated with aggressive disease and worse patient outcome (31). It should be noted that the quantitative RT-PCR assay detects other splice variants, particularly the C4 variant, which may also contribute to the observed correlation, although the C5 variant was the most highly expressed form. Although the spliced variant mRNA are only a portion of total CDC25C mRNA in vivo, it may have significant biological effects that lead to more aggressive diseases, perhaps through poor regulation of its activity. Thus, prostate cancer is characterized by multiple alterations in CDC25C that can increase its activity *in vivo*.

Based on comparison of CDC25C and Ki-67 transcript levels, there was a significant correlation of WT and variant CDC25C transcript levels with Ki-67 transcript levels. Increased expression of CDC25C would be expected to promote progression through the G2/M checkpoint and, particularly if associated with loss of other cell cycle checkpoint controls, would increase cellular proliferation. Further mechanistic studies to determine the basis of the increased CDC25C transcript levels in cancer may reveal

whether this is a primary event associated with malignant transformation or a secondary event related other alterations in prostate cancer cells such as increased growth factor signaling.

The finding that the level of alternatively spliced CDC25C transcripts is correlated with recurrence, even after correction for proliferation by normalization to Ki-67 levels indicates that expression of variant CDC25C has independent correlation with biochemical recurrence. Bureik et al. (19) have shown that expression of the major alternatively spliced CDC25C variant in *S. Pombe* resulted in uncoupling of mitosis from completion of S-phase. Of note is the finding that the C5 variant does not appear to be phosphorylated at the inhibitory serine 216 residue. This site is phophorylated by Chk kinase, which plays an important role in protecting the genomic integrity of cells following DNA damage (32). Thus expression of the C5 variant of CDC25C could potentially result in genomic instability, which could facilitate emergence of aggressive disease. Further studies are needed to test this possibility.

In summary, we have described, for the first time, the increased activity of CDC25C phosphatase and overexpression of an alternatively spliced CDC25C mRNA in prostate cancer. Increased expression of the both total CDC25C mRNA and its spliced variant are correlated with biochemical recurrence, particularly early recurrence. Further studies need to be done to determine the role of CDC25C and its spliced variants in prostate cancer pathogenesis.

ACKNOWLEDGEMENTS

This work was supported by a grant from the Department of Defense Prostate Cancer Research Program (DAMD17-03-1-0006; M. Ozen), by Merit Review funding from the Dept of Veterans Affairs (M. Ittmann), by a grant to the Baylor prostate cancer SPORE program from the National Cancer Institute (P50CA058204) and by an award from the Moran Foundation. This work was also supported by the use of the facilities of the Michael E. DeBakey VAMC.

REFERENCES

1. Mashal, R. D., Lester, S., Corless, C., Richie, J. P., Chandra, R., Propert, K. J., and Dutta, A. Expression of cell cycle-regulated proteins in prostate cancer. Cancer Research, *56*: 4159-4163, 1996.

2. Kallakury, B. V., Sheehan, C. E., Ambros, R. A., Fisher, H. A., Kaufman, R. P., Muraca, P. J., and Ross, J. S. Correlation of p34(cdc2) cyclin-dependent kinase overexpression, CD44s downregulation, and HER-2/neu oncogene amplification with recurrence in prostatic adenocarcinomas. Journal of Clinical Oncology, *16*: 1302-1309, 1998.

3. Maddison, L. A., Huss, W. J., Barrios, R. M., and Greenberg, N. M. Differential expression of cell cycle regulatory molecules and evidence for a "cyclin switch" during progression of prostate cancer. Prostate, *58*: 335-344, 2004.

4. Booher, R. N., Holman, P. S., and Fattaey, A. Human Myt1 is a cell cycle-regulated kinase that inhibits Cdc2 but not Cdk2 activity. Journal of Biological Chemistry, *272*: 22300-22306, 1997.

5. Draetta, G. and Eckstein, J. Cdc25 protein phosphatases in cell proliferation. Biochimica et Biophysica Acta-Reviews on Cancer, *1332*: M53-M63, 1997.

6. Taylor, W. R. and Stark, G. R. Regulation of the G2/M transition by p53. Oncogene, *20*: 1803-1815, 2001.

7. Ozen, M., Giri, D., Ropiquet, F., Mansukhani, A., and Ittmann, M. Role of fibroblast growth factor receptor signaling in prostate cancer cell survival. Journal of the National Cancer Institute, *93*: 1783-1790, 2001.

8. Turowski, P., Franckhauser, C., Morris, M. C., Vaglio, P., Fernandez, A., and Lamb, N. J. C. Functional cdc25C dual-specificity phosphatase is required for S-phase entry in human cells. Molecular Biology of the Cell, *14*: 2984-2998, 2003.

9. Graves, P. R., Lovly, C. M., Uy, G. L., and Piwnica-Worms, H. Localization of human Cdc25C is regulated both by nuclear export and 14-3-3 protein binding. Oncogene, *20*: 1839-1851, 2001.

10. Dunphy, W. G. and Kumagai, A. The Cdc25 Protein Contains An Intrinsic Phosphatase-Activity. Cell, *67*: 189-196, 1991.

11. Strausfeld, U., Labbe, J. C., Fesquet, D., Cavadore, J. C., Picard, A., Sadhu, K., Russell, P., and Doree, M. Dephosphorylation and Activation of A P34Cdc2 Cyclin-B Complex Invitro by Human Cdc25 Protein. Nature, *351*: 242-245, 1991.

12. Graves, P. R., Yu, L. J., Schwarz, J. K., Gales, J., Sausville, E. A., O'Connor, P. M., and Piwnica-Worms, H. The Chk1 protein kinase and the Cdc25C regulatory pathways are targets of the anticancer agent UCN-01. Journal of Biological Chemistry, *275*: 5600-5605, 2000.

13. Peng, C. Y., Graves, P. R., Thoma, R. S., Wu, Z. Q., Shaw, A. S., and PiwnicaWorms, H. Mitotic and G(2) checkpoint control: Regulation of 14-3-3 protein binding by phosphorylation of Cdc25C on serine-216. Science, *277*: 1501-1505, 1997.

14. Hoffmann, I. The role of Cdc25 phosphatases in cell cycle checkpoints. Protoplasma, *211*: 8-11, 2000.

15. Izumi, T. and Maller, J. L. Phosphorylation and Activation of the Xenopus Cdc25 Phosphatase in the Absence of Cdc2 and Cdk2 Kinase-Activity. Molecular Biology of the Cell, *6*: 215-226, 1995.

16. Zeng, Y., Forbes, K. C., Wu, Z. Q., Moreno, S., Piwnica-Worms, H., and Enoch, T. Replication checkpoint requires phosphorylation of the phosphatase Cdc25 by Cds1 or Chk1. Nature, *395*: 507-510, 1998.

17. Baldin, V., Cans, C., SupertiFurga, G., and Ducommun, B. Alternative splicing of the human CDC25B tyrosine phosphatase. Possible implications for growth control? Oncogene, *14*: 2485-2495, 1997.

18. Wegener, S., Hampe, W., Herrmann, D., and Schaller, H. C. Alternative splicing in the regulatory region of the human phosphatases CDC25A and CDC25C. European Journal of Cell Biology, *79*: 810-815, 2000.

19. Bureik, M., Rief, N., Drescher, R., Jungbluth, A., Montenarh, M., and Wagner, P. An additional transcript of the cdc25C gene from A431 cells encodes a functional protein. International Journal of Oncology, *17*: 1251-1258, 2000.

20. Giri, D., Ropiquet, F., and Ittmann, M. FGF9 is an autocrine and paracrine prostatic growth factor expressed by prostatic stromal cells. Journal of Cellular Physiology, *180*: 53-60, 1999.

21. Polnaszek, N., Kwabi-Addo, B., Peterson, L. E., Ozen, M., Greenberg, N. M., Ortega, S., Basilico, C., and Ittmann, M. Fibroblast growth factor 2 promotes tumor progression in an autochthonous mouse model of prostate cancer. Cancer Research, *63*: 5754-5760, 2003.

22. Kwabi-Addo, B., Wang, J. H., Erdem, H., Vaid, A., Castro, P., Ayala, G., and Ittmann, M. The expression of sprouty1, an inhibitor of fibroblast growth factor signal transduction, is decreased in human prostate cancer. Cancer Research, *64*: 4728-4735, 2004.

23. Galaktionov, K., Lee, A. K., Eckstein, J., Draetta, G., Meckler, J., Loda, M., and Beach, D. Cdc25 Phosphatases As Potential Human Oncogenes. Science, *269*: 1575-1577, 1995.

24. Gasparotto, D., Maestro, R., Piccinin, S., Vukosavljevic, T., Barzan, L., Sulfaro, S., and Boiocchi, M. Overexpression of CDC25A and CDC25B in head and neck cancers. Cancer Research, *57*: 2366-2368, 1997.

25. Wu, W. G., Fan, Y. H., Kemp, B. L., Walsh, G., and Mao, L. Overexpression of cdc25A and cdc25B is frequent in primary non-small cell lung cancer but is not associated with overexpression of c-myc. Cancer Research, *58*: 4082-4085, 1998.

26. Kudo, Y., Yasui, W., Ue, T., Yamamoto, S., Yokozaki, H., Nikai, H., and Tahara, E. Overexpression of cyclin-dependent kinase-activating CDC25B phosphatase in human gastric carcinomas. Japanese Journal of Cancer Research, *88*: 947-952, 1997.

27. Hernandez, S., Bessa, X., Bea, S., Hernandez, L., Nadal, A., Mallofre, C., Muntane, J., Castells, A., Fernandez, P. L., Cardesa, A., and Campo, E. Differential expression of cdc25 cell-cycle-activating phosphatases in human colorectal carcinoma. Laboratory Investigation, *81*: 465-473, 2001.

28. Guo, J. C., Kleeff, J., Li, J. S., Ding, J. Y., Hammer, J., Zhao, Y. P., Giese, T., Korc, M., Buchler, M. W., and Friess, H. Expression and functional significance of CDC25B in human pancreatic ductal adenocarcinoma. Oncogene, *23*: 71-81, 2004.

29. Ngan, E. S. W., Hashimoto, Y., Ma, Z. Q., Tsai, M. J., and Tsai, S. Y. Overexpression of Cdc25B, an androgen receptor coactivator, in prostate cancer. Oncogene, *22*: 734-739, 2003.

30. Tsuda, H., Hashiguchi, Y., Inoue, T., and Yamamoto, K. Alteration of G2 cell cycle regulators occurs during carcinogenesis of the endometrium. Oncology, *65*: 159-166, 2003.

31. Swindle, P. W., Kattan, M. W., and Scardino, P. T. Markers and meaning of primary treatment failure. Urologic Clinics of North America, *30*: 377-+, 2003.

32. Lam, M. H., Liu, Q. H., Elledge, S. J., and Rosen, J. M. Chk1 is haploinsufficient for multiple functions critical to tumor suppression. Cancer Cell, *6*: 45-59, 2004.

FIGURE LEGENDS:

Figure 1. CDC25C protein levels in clinically localized human prostate cancers.

Normal peripheral zone and cancer tissues were collected from men undergoing radical prostatectomy for clinically localized prostate cancer by Baylor prostate cancer SPORE Tissue Core and snap frozen. Protein lysates were prepared as described in "Materials and Methods". Western blot for CDC25C was performed using polyclonal anti-CDC25C antibody or a serine 216 phosphorylation site specific antibody. An anti-β-actin monoclonal antibody was used as loading control. The numbers representing samples are obtained from our clinical database. Sample 24 was not included in the analysis due to low β-actin signal, indicating inadequate protein in this lane.

Figure 2. Expression of full length and alternatively spliced CDC25C mRNA and/or proteins in prostate tissues and prostate cancer cell lines.

(A) RNAs were extracted from normal peripheral zone tissues, BPH tissues and prostate cancer tissue samples using TRIzoL Reagent as described by the manufacturer's protocol and analyzed by RT-PCR as described in Materials and Methods. Bands corresponding to the full length (512 bp) and variant mRNA (293 bp) are indicated. Three samples each of cancer, normal and BPH groups are shown. RT-PCR with β-actin primers was used as a control for cDNA quantity.

(B) Protein lysates from prostate cancer cell lines are subjected to Western blot analysis using the appropriate antibodies as described in "Materials and Methods". Preincubation

with peptide immunogen for the CDC25C antibody was used to determine the specificity of the two CDC25C bands.

Figure 3. Correlation of PSA recurrence with expression of CDC25C mRNAs relative to β-actin as determined by real time RT-PCR. Total and WT mRNA transcript levels were determined by quantitative RT-PCR as described in Materials and Methods. Alternatively spliced transcript levels were calculated by subtraction of wild type CDC25C transcript levels from the total CDC25C levels. Mean values are shown +/- standard error. Statistically significant differences are marked with an asterisk.

Figure 4. Correlation of expression of Ki-67 mRNA relative to β-actin with clinical and pathological parameters in clinically localized prostate cancer. Clinical samples are grouped by Gleason grade, presence of extracapsular extension (ECE), seminal vesicle invasion (SVI) and lymph node metastasis (LN Met). Cases with PSA recurrence were compared to those without recurrence (-). Statistically significant differences are indicated by an asterisk.

Figure 5. Relative expression of CDC25C to Ki67 in prostate cancer. Total and WT mRNA transcript levels were determined by quantitative RT-PCR as described in Materials and Methods. Alternatively spliced transcript levels were calculated by subtraction of wild type CDC25C transcript levels from the total CDC25C levels. Samples are grouped by their recurrence status and interval. Statistically significant differences in each group are marked with an asterisk.

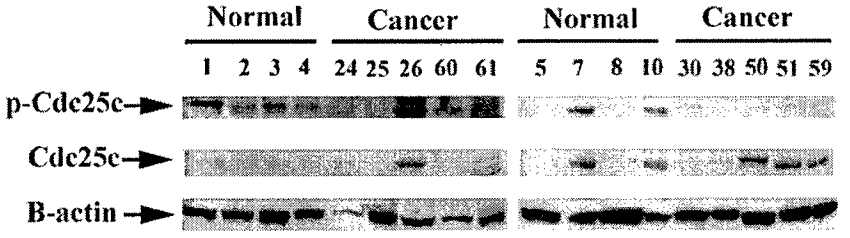
Normal
Cancer
Normal
Cancer
1 2 3 4 24 25 26 60 61 5 7 8 10 30 38 50 51 59
p-Cdc25c
Cdc25c
B-actin

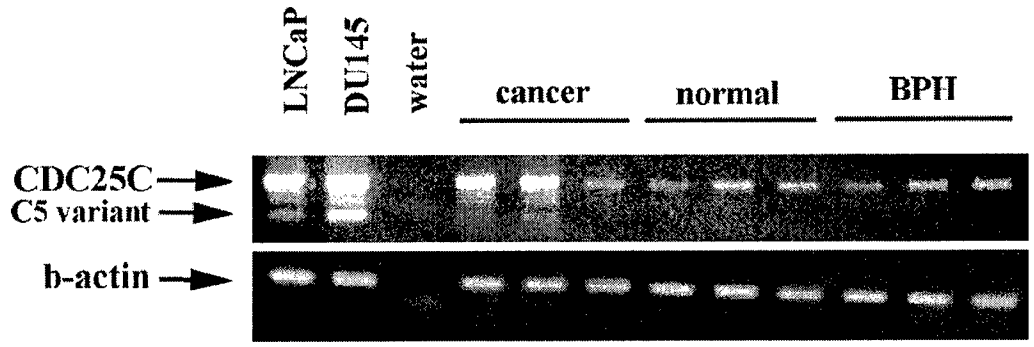
LNCaP
DU145
water
cancer
normal
BPH
CDC25C
C5 variant
b-actin

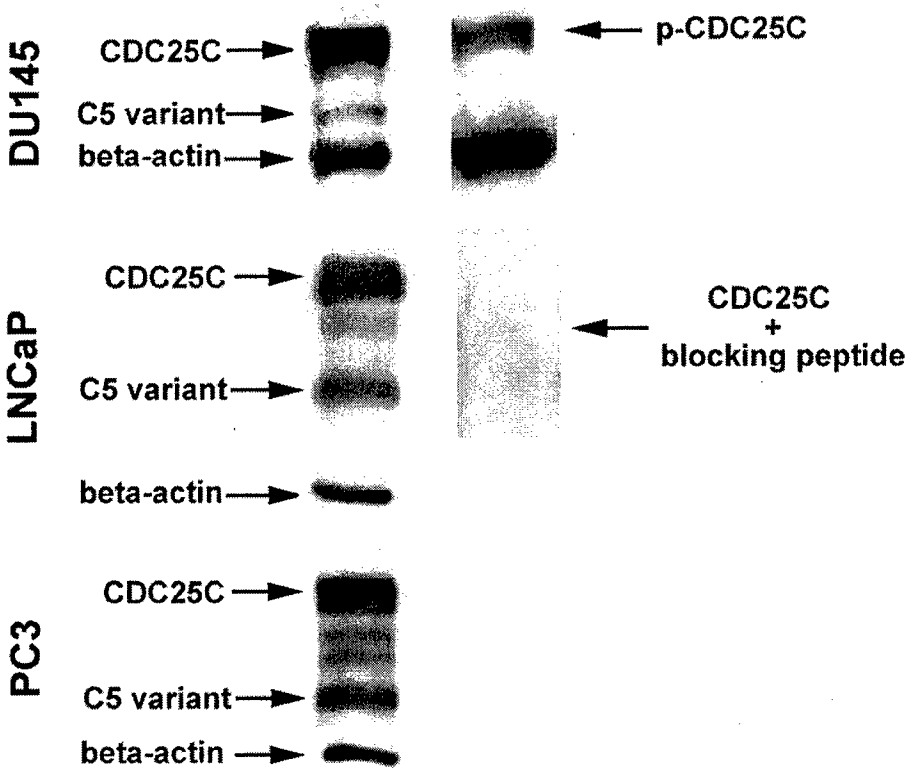
DU145
CDC25C
C5 variant
beta-actin
p-CDC25C
LNCaP
CDC25C
C5 variant
beta-actin
CDC25C
+
blocking peptide
PC3
CDC25C
C5 variant
beta-actin

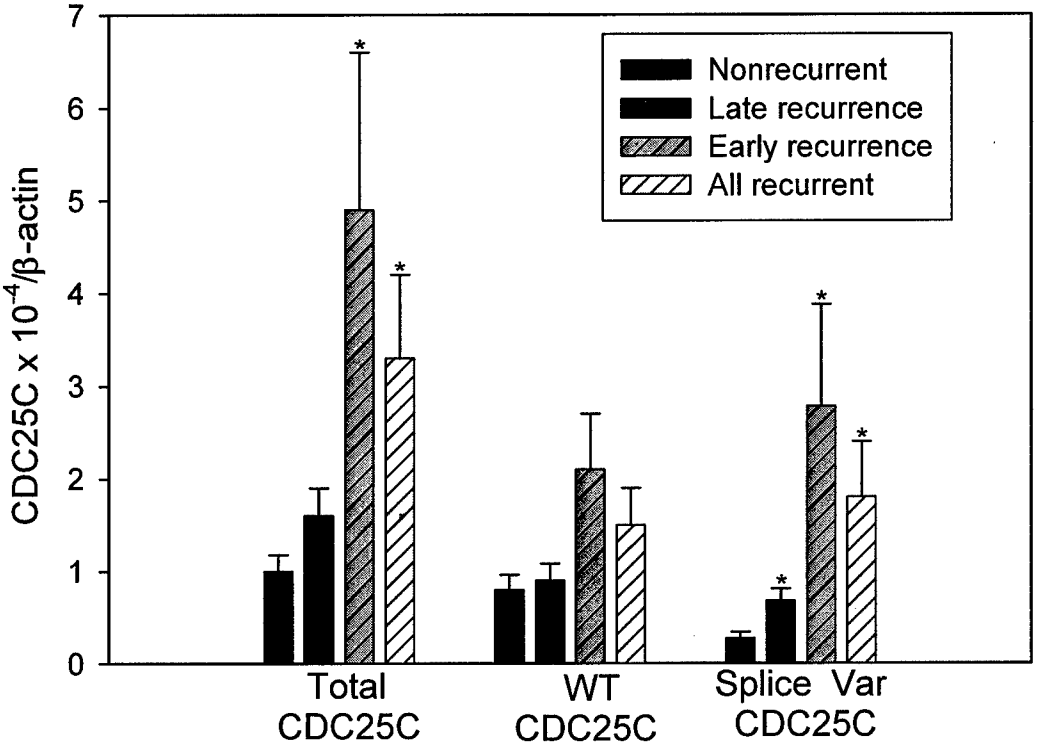
CDC25C x 10^{-4}/β-actin
7
6
5
4
3
2
1
0
Nonrecurrent
Late recurrence
Early recurrence
All recurrent
*
*
*
*
Total CDC25C
WT CDC25C
Splice Var CDC25C

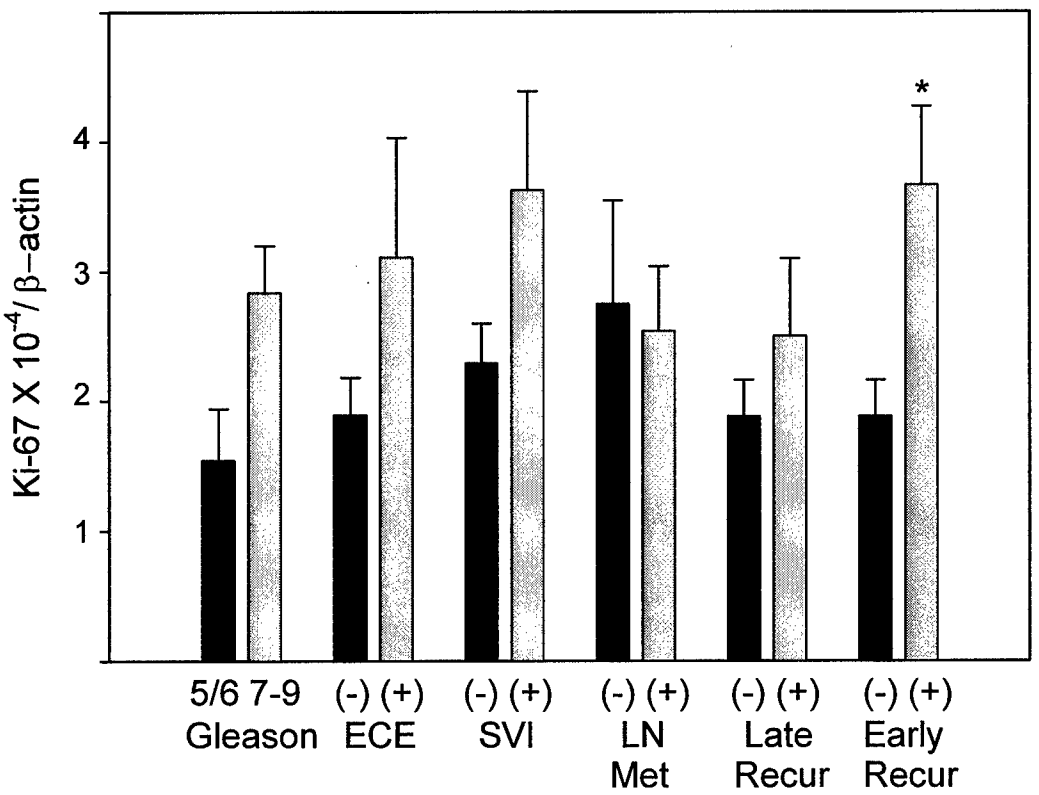
Ki-67 X 10^{-4}/β–actin
4
3
2
1
*
5/6 7-9
Gleason
(-) (+)
ECE
(-) (+)
SVI
(-) (+)
LN
Met
(-) (+)
Late
Recur
(-) (+)
Early
Recur

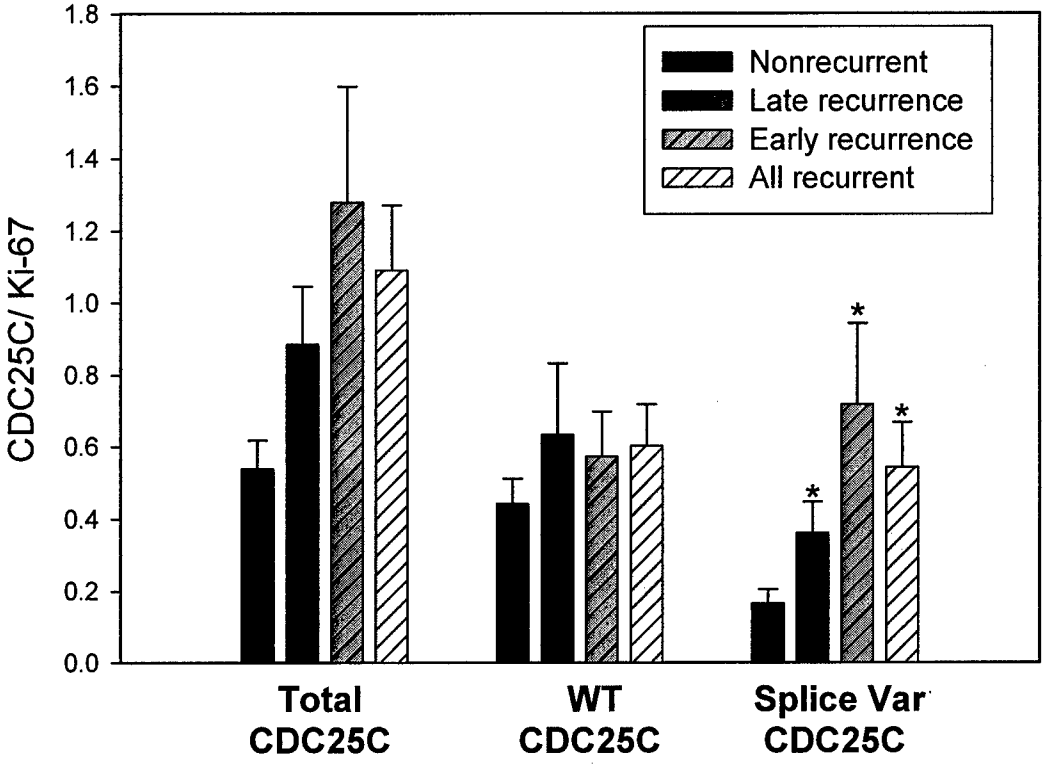
1.8
1.6
1.4
1.2
1.0
0.8
0.6
0.4
0.2
0.0
CDC25C/ Ki-67
Nonrecurrent
Late recurrence
Early recurrence
All recurrent
*
*
*
Total CDC25C
WT CDC25C
Splice Var CDC25C

Mustafa Ozen

From: Michael Ittmann [mittmann@bcm.tmc.edu]
Sent: Friday, April 01, 2005 2:37 PM
To: mozen@bcm.tmc.edu
Subject: FW: Manuscript CCR-04-2551 Version 2

-----Original Message-----
From: ccr@aacr.org [mailto:ccr@aacr.org]
Sent: Friday, April 01, 2005 10:38 AM
To: mittmann@bcm.tmc.edu
Subject: Manuscript CCR-04-2551 Version 2

Dr. Michael M. Ittmann
Baylor College of Medicine
Research Service
Houston VAMC
2002 Holcombe Blvd
Houston, TX
United States
77030

Dear Dr. Ittmann:

I am pleased to inform you that your manuscript entitled Increased expression and activity of CDC25C phosphatase and an alternatively spliced variant in prostate cancer., CCR-04-2551 Version 2, has been accepted for publication in CLINICAL CANCER RESEARCH. You will be informed of the scheduled publication date shortly.

You will receive page proofs within approximately 12-14 weeks. If your manuscript submission information included an e-mail address, you will receive electronic page proofs. If you do not have access to e-mail, you will receive hard copy page proofs. If you expect your contact information to change within the next few weeks, please contact the
Editorial Office immediately either by e-mail to ccr@aacr.org, or by fax to (215)440-9354.

We would like to call your particular attention to the following:

1) When page proofs are received, please read, correct, and put them in the mail to the Editorial Office, American Association for Cancer Research 615 Chestnut St., 17th Floor Philadelphia, PA 19106-4404, WITHIN 24 HOURS. Page proofs should be returned by the FASTEST MAIL SERVICE AVAILABLE. Weekend delivery is not necessary, as our schedule takes weekends and holidays into account.
IMPORTANT: PLEASE NOTE THAT IF PROOFS ARE NOT RETURNED WITHIN THIS TIMEFRAME, PUBLICATION OF THE ARTICLE MAY BE POSTPONED UNTIL THE NEXT AVAILABLE ISSUE.

2) Changes in proofs entail considerable expense and publication delay and thus are discouraged unless absolutely necessary. Authors will be charged for excessive alterations made in proof.

3) When reading proofs, please answer carefully all of the copy editor's queries, and pay particular attention to the illustrations to ensure the quality and accuracy of their reproduction. Please read the entire manuscript carefully to verify that no changes in meaning have been introduced through copy editing.

4) Retain a copy of your corrected proof in the event that the original is lost or delayed in the mail.

Thank you in advance for your cooperation.

Sincerely,

Arnold B. Rabson, M.D.
Senior Editor

ST22. Increased CDC25C Phosphatase Activity in Prostate Cancer: Correlation To Biochemical Recurrence*

Mustafa Ozen and Michael Ittmann, Department of Pathology, Baylor College of Medicine and Michael E. DeBakey, Dept. of Veterans Affairs Medical Center, Houston, Texas 77030.

Alterations in proteins regulating cell cycle progression have been implicated in the pathogenesis in a wide variety of malignant neoplasms, including prostate cancer. CDC25 phosphatases belong to the tyrosine phosphatase family and play a critical role in regulating cell cycle progression by dephosphorylating cyclin dependent kinases at inhibitory residues. CDC25C plays an important role in the G2/M transition by activating Cdc2/Cyclin B1 complexes. To determine whether CDC25C activity is altered in prostate cancer, we have examined the expression of CDC25C and its alternatively spliced variant in human prostate cancer. CDC25C protein is upregulated in prostate cancer in comparison to normal prostate tissue and is present almost exclusively in its active dephosphorylated form. Expression of a biologically active alternatively spliced CDC25C isoform is also increased in prostate cancer and is correlated with the occurrence of biochemical (PSA) recurrence. This data suggest that CDC25C might play an important role in prostate cancer progression and could be used to monitor and predict the aggressiveness of this disease. *This work was supported by grant from the Department of Defense Prostate Cancer Research Program (DAMD17-03-1-0006).

ST24. Clinical and Molecular Characteristics of Pediatric Gastrointestinal Stromal Tumors (GISTs)

Susan Chilton-MacNeill, Victoria Price, Charles Smith, Alberto Pappo, Maria Zielenska, Hospital for Sick Children, Toronto, ON, Canada.

GISTs are the most common mesenchymal tumors of the gastrointestinal tract in adults and are characterized by c-KIT expression (CD117) and exon 11 mutations. The natural history and molecular characteristics of these tumors in children are unknown.A study of 6 patients with GIST was undertaken to describe clinical characteristics, treatment, outcome and molecular features. c-KIT expression of these tumors was determined by immunchistochemistry and mutational status evaluated in c-kit exon 9, 11 and 13. The median age of patients at diagnosis was 13.6 years. Iron deficiency anaemia secondary to gastrointestinal hemorrhage was a presenting feature in all patients. The primary site was the stomach. Five patients presented with localized disease. Two patients had evidence of Carneys triad. All tumors were positive for CD117. Three samples were available for molecular analysis. No sequence abnormalities were found in exons 11 and 13. A novel point mutation in exon 9 was found in one patient. All of the tumors were surgically resected and none of the patients received chemotherapy. Disease recurred in 1 patient, 2 were lost to follow-up, and 4 remain alive.GISTs should be considered in the differential diagnosis of pediatric patients presenting with anaemia secondary to gastrointestinal hemorrhage. GISTs in the pediatric population preferentially arise in the stomach, and do not exhibit an exon 11 c- kit mutation. The latter findings suggest that pediatric GISTs may have biological differences compared to adult GISTs. Multicenter studies are needed to elucidate the natural history, molecular phenotype, and therapies for these patients.

ST25. CpG Island Methylation Profile in Gastric Carcinoma

Alejandro Corvalan, Claudia Backhouse, Ignacio Wistuba, Francisco Aguayo, Miguel A. Cumsille, Mariana Palma, Erick Riquelme, Jorge Argandona, Victor Luengo, Suminori Akiba, Chihaya Koriyama, Yoshito Eizuru., Department of Pathology, Catholic University and Institute for Digestive Disease and School of Public Health University of Chile, Santiago Chile, MD Anderson Cancer Center Houston TX USA, Department Public Health Kagoshima University, Kagoshima Japan.

Background: Gastric carcinoma (GC) is one of the most common neoplasms in the world and has been associated with CpG island methylation (CIM). However, associations between clinico-pathological characteristics, prognostic features and precursor lesions of GC and CIM are not well understood. **Methods:** Methylation status of 14 tumor suppressor genes was investigated using methylation-specific polymerase chain reaction in 94 cases of GC and 33 corresponding adjacent non-neoplastic mucosa. Frequencies of methylation were compared by methylation index (MI, total number of genes methylated divided by the total number of genes analyzed). **Results:** In GC methylation frequencies varied from 1.1% to 67%. Four genes demonstrated relatively high frequencies of aberrant methylation (>40%): BRCA1, p14, APC, p16. Four genes showed intermediate frequencies (10-40%): MGMT, p15, p73 and DAPK and six genes showed low frequencies (<10%): TIMP-3, GSTp, ER, RARbeta, hMLH1 and SOCS. MI was significant increase in intestinal-type GC (p=0.041), specifically p14 and p16 genes (p=0.0001). No other clinico-pathological characteristics (gender, age, tumor size, stage, lymph node metastasis, EBV infection and MSI) were associated with CIM. Hypermethylated APC was associated with reduced survival in diffuse-type GC (p=0.029) and hypermethylated BRCA1 was detected in 16 (48.9%) of 33 corresponding non-neoplastic mucosa. **Conclusions:** CIM is a frequent event in gastric tumorigenesis, and associated with specific clinico-pathological characteristics and prognostic features. Methylation of the BRCA1 gene may contribute to the malignant transformation of gastric precursor lesions. Evaluation of CpG island methylation in serum samples might be useful for early detection of GC. Supported by Grant FONDECYT Chile 1030130 (A.C.)

ST26. Molecular Discrimination of Benign and Malignant Esophageal Tissues Using Multi-Marker Real-Time RT-PCR

Michael Mitas[1], Kaidi Mikhitarian[1], Jonas S. Almeida [2], William E. Gillanders[1], David N. Lewin[3], Demetri D. Spyropoulos[3], Loretta Hoover[1], Angela Collier[1], Amanda Graham[1], David Robbins[4], Peter King[4], David J. Cole[1], Carolyn E. Reed[1], and Brenda J. Hoffman[1], [1]Department of Surgery, Medical University of South Carolina [2]Department of Biometry & Epidemiology, Medical University of South Carolina [3]Pathology & Laboratory Medicine, Medical University of South Carolina [4]Digestive Disease Center, Medical University of South Carolina.

Esophageal adenocarcinoma (EA) is increasing faster than any other cancer in the US. For the ultimate purpose of developing a reliable assay for early detection of esophageal malignancies, we determined the expression levels of 14 cancer-associated genes in various esophageal tissues by quantitative real-time RT-PCR. Of the genes tested, we identified three that had unique and highly accurate (area under the receiver operator curve value >0.97) discrimination capabilities: *epithelial cell adhesion molecule* (*EpCam*) discriminates between normal esophagus (NE)/Barrett's esophagus (BE) and esophageal adenocarcinoma (EA), *trefoil factor 1* (*TFF1*) discriminates between EA and esophageal squamous cell carcinoma (ESCC), and *small breast epithelial molecule* (*SBEM*) discriminates between NE and ESCC. Based on results using training (n=53) and test (n=17) samples, we show that a plot of expression values for *EpCam*, *TFF1*, and *SBEM* in three-dimensional Euclidean space allows for accurate classification (overall accuracy = 68/70, 97%) of esophageal tissues. To assess the value of the three-gene marker assay for early detection of EA, we analyzed high-grade dysplasia (HGD) samples (n=4). All HGD samples were molecularly classified as EA, providing evidence that this condition, considered by many to be premalignant, can be detected by molecular methods and is characterized by overexpression of *EpCam* and *TFF1*. Further studies are needed to determine whether the assay described in this paper will be of value for monitoring or predicting progression of BE to EA.

ST27. Screening for EGFR Mutations Predicting Response to Targeted Therapy

Mezgebe Gebrekiristos, Lela Buckingham, Philip Bonomi and John S. Coon, Rush University Medical Center, Chicago, IL.

Dramatic response of lung cancer patients to the tyrosine kinase inhibitor, Iressa (Gefitinib; ZD1839) has been observed in only about 10% of treated patients. Sequence analyses have shown that response varies with the presence of specific mutations in the catalytic domain of the EGFR kinase, specifically, exons 18, 19 and 21. Using the single strand conformation polymorphism (SSCP) method, we have tested tumors from lung cancer patients with stable disease, progressive disease or partial response after treatment with Iressa. SSCP is a relatively simple and rapid method that has been used extensively to screen for DNA mutations. None of 10 control patients with progressive disease had mutations in exons 18, 19 or 21 of the EGFR gene, while 6 of 9 patients with stable disease or partial response had mutations. Consistent with previous reports that described sequence changes favorable to response, the SSCP analysis revealed point mutations in exon 18 and deletions in exon 19. With sequence confirmation of specific base changes, specific band patterns for given mutations can be interpreted as specific mutations. This method offers a simple, cost effective way to screen for clinically significant mutations in the EGFR gene.

ST28. Comparison of FISH and Cytology for the Detection of Lung Cancer in Bronchoscopically Obtained Brushing and Secretion Specimens

Aaron R. Herwood, Otis B. Rickman, James R. Jett, Kevin C. Halling, Depts. of Laboratory Medicine and Pathology, Pulmonary and Critical Care Medicine, Mayo Clinic, Rochester, MN.

In 2004 lung cancer will cause more deaths than prostate, breast, colon and pancreatic cancer combined due to advanced stage of disease at diagnosis. This study analyzed the utility of fluorescence in situ hybridization (FISH) using the LAVysion® probe set (contains probes to centromere 6, 5p15, 8q24[*C-MYC*] and 7p12[*EGFR*]) to detect lung cancer in comparison to conventional cytology. The relative sensitivity and specificity of FISH and cytology on bronchial brushings and secretions from 104 patients suspected of having lung cancer were assessed. Using bronchoscopic biopsy as the gold standard, the relative sensitivity of FISH and cytology on brushings was 75.0% (30/40) and 50.0% (20/40) (p<0.05) respectively. The relative sensitivity of FISH and cytology on secretions was 45.5% (20/44) and 43.2% (19/44) (p=NS) respectively. The specificity of FISH and cytology on brushings for patients with negative biopsies at the time of FISH and cytology was 64.3% (18/28) and 92.6% (25/27) (p=NS) respectively. However, extended follow-up of the 10 "false-positive" FISH brushing results showed that 5 patients were subsequently diagnosed with lung cancer (tissue diagnosis). Based on this, the re-adjusted specificity of FISH and cytology for the bronchial brushings was 81.8%. The specificity of FISH and cytology on the secretions was 93.0% (28/30) and 100% (30/30) (p=NS) respectively. These results suggest that FISH is more sensitive than conventional cytology on brushing samples and similarly sensitive on secretion specimens and that FISH with LAVysion® may be able to detect lung cancer before it is evident by other means.